Austrian Society for ASEM Electron Microscopy

Zentrum für Oberflächen- und Nanoanalytik

11th ASEM workshop

Advanced Electron Microscopy

May 20th – May 21st, 2021

Host: ZONA, JKU Linz
via ZOOM

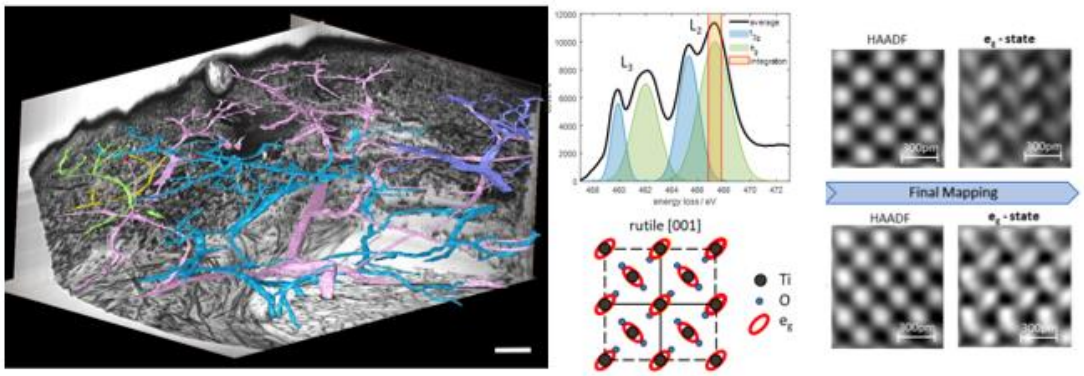

Abstract book

Programm

	Donnerstag 20. Mai 2021
09:30 Uhr	ASEM Vorstandssitzung
09:45 Uhr	
10:00 Uhr	
10:15 Uhr	
10:30 Uhr	**Eröffnung**
10:45 Uhr	EMCD on Antiferromagnets - Stefan Löffler, TU Wien
11:00 Uhr	CCLEM – ZEISS new 3D Multi-Scale Correlative Cryo Light and Electron Microscopy Workflow for Cryo-TEM Lamella Preparation - Wolfgang Schwinger, ZEISS
11:15 Uhr	Atomic-scale characterization of interface and microstructure of bilayer TaN/TiN thin films on different substrates -Yong Huang, ESI Leoben
11:30 Uhr	3D Nanoprinting with Electrons - From Meshes to Closed Structures - Anna Weitzer, FELMI-ZFE
11:45 Uhr	Efficient Particles Size Distribution Characterization with TEM: Recent Advances in Experiments and Analysis Automation - Daniel Stroppa, ThermoScientific
12:00 Uhr	**Lunch break**
12:15 Uhr	
12:30 Uhr	
12:45 Uhr	
13:00 Uhr	
13:15 Uhr	
13:30 Uhr	**Poster session**
13:45 Uhr	
14:00 Uhr	Sub 50nm Transmission Kikuchi Diffraction (TKD) of a TiAlNb TEM lamella using a modern FE-SEM and EBSD system - Berhard Bichler, Videko-HITACHI
14:15 Uhr	Sample Preparation in Plan-View Geometry for In Situ TEM Heating Experiments - Natalie Santic, JKU Linz
14:30 Uhr	Towards Damage-Free Molecular Movies with Optical Near-Field Electron Microscopy - Raphael Marchand - Uni Wien
14:45 Uhr	In situ Transmission Scanning Electron Microscopy as a Tool to Resolve Interface Related Deformation and Fracture in Multilayered Components - Markus Alfreider, MU Leoben
15:00 Uhr	Influence of primary beam energy on localized surface plasmon resonances mapping by STEM-EELS - Michal Horak, CEITEC Brno
15:15 Uhr	Complexion Formation in Solid Oxide Cells - Inter-Diffusion across the Electrode/Electrolyte interface - Franz-Philipp Schmidt, FHI Berlin
15:30 Uhr	**Pause**
15:45 Uhr	
16:00 Uhr	Establishing Organotypic Culture as a Model System to Study the Iron Homeostasis in Human Neurodegenerative Diseases in the Central Nervous System - Sowmya Sunkara, MedUni Graz
16:15 Uhr	Expanding Design Possibilities by Blurred Electron Beams during 3D Nanoprinting - Lukas Seewald, TU Graz
16:30 Uhr	High Resolution STEM Simulations of Beryl Crystal Impurities Using Multislice Methods (QSTEM) - Nikola Simic, FELMI-ZFE
16:45 Uhr	Multimodal & Multiscale materials characterization in battery research: the game changer Xe plasma FIB-SEM - Tom Jäpel, Tescan
17:00 Uhr	"Flash and Freeze" in Brain Slices: Structure-Function Analysis of Synapses in the Central Nervous System by Electron Microscopy - Carolina Borges Meerjane & Olena KIM, IST Austria
17:15 Uhr	
17:30 Uhr	**Pause**
17:45 Uhr	
18:00 Uhr	**ASEM Hauptversammlung**
18:15 Uhr	
18:30 Uhr	
18:45 Uhr	
	Freitag 21. Mai 2021
09:00 Uhr	In-situ TEM Investigation of Toughening in Silicon at Small Scales - Inas Issa, MU Leoben
09:15 Uhr	
09:30 Uhr	Imaging the Spatial Distribution of π* States In Graphene - Manuel Ederer, TU Wien
09:45 Uhr	Relationship of Microstructure and Magnetic Domain Configuration of a Spinodally Decomposed Cu52Ni34Fe14 Alloy - Thomas Radlinger, TU Graz
10:00 Uhr	The JSM-IT800 series - The next level of Intelligence Technology in FE-SEM combining ultrahigh resolution and unprecedented ease of use - Georg Raggl, JEOL
10:15 Uhr	MEMS-based in situ Electron-Microscopy Investigation of Rapid Solidification and Heat Treatment on Eutectic Al-Cu - Phillip Dumitraschkewitz, MU Leoben
10:30 Uhr	**Pause**
10:45 Uhr	
11:00 Uhr	In situ TEM Study of Sn-Ge Nanosystem Thermal Stability - Alexej Minkenov, ZONA Linz
11:15 Uhr	High Pressure Freezing and Glycan Microarray Analysis Indicate High Resistance of Green Algal Mougeotia and Spirogyra Zygospores - Charlotte Permann, Uni Innsbruck
11:30 Uhr	The Impact of High-Tension on the Orbital Mapping of Rutile by STEM-EELS - Michael Oberaigner, TU Graz
11:45 Uhr	Reconstructing Parent Microstructures from EBSD based Orientation Measurements - Rene de Kloe, EDAX AMETEC
12:00 Uhr	**Lunch break**
12:15 Uhr	
12:30 Uhr	
12:45 Uhr	
13:00 Uhr	
13:15 Uhr	
13:30 Uhr	In-situ Nanoscale Characterization of Electrical and Magnetic properties of 3D Nanostructures by combination of AFM, SEM and FIB - Christian Schwalb, GeTEC
13:45 Uhr	In-situ atomic-resolution observation of coherent twin boundary migration in CrN - Chen Zuo, ESI Leoben
14:00 Uhr	Advancements in segmentation of 3D SEM images of neurons: pre-processing steps - Snježana Radulović, MedUni Graz
14:15 Uhr	Implications of Low Substrate Temperatures on Growth Dynamics during 3D Nanoprinting via Electrons - Jakob Hinum-Wagner, TU Graz
14:30 Uhr	Fusion of mitochondria to 3-D networks, autophagy and increased organelle contacts are important subcellular hallmarks during cold stress in plants - Philip Steiner, JKU Linz
14:45 Uhr	
	Closing remarks

VORTRÄGE

EMCD on Antiferromagnets

Stefan Löffler[1], Fabian Spies[2] and Michael Stöger-Pollach[1]

1 University Service Centre for Transmission Electron Microscopy, TU Wien, Wien, Austria
2 Institute of Solid State Physics, TU Wien, Wien, Austria

Energy-loss magnetic chiral dichroism (EMCD) is a powerful EELS technique to study magnetism down to the atomic scale [1]. It is based on the fact that inelastic scattering in magnetic materials produces electron vortex beams (EVBs), which can be measured interferometrically. Conventionally, crystalline materials are used, which act as specimen (creating the EVBs) and interferometry device (beam splitter/phase manipulator) at the same time. Usually, incident plane waves are used for EMCD. This effectively prevents the characterization of antiferromagnetic samples, since the signals of spin-up and spin-down atoms average out.

Here, we present numerical simulations investigating the possibility of using convergent beam EMCD [2] to solve the problem of signal averaging. As a model system, we used NiO in systematic row condition including the (1 1 -1) spot such that adjacent Ni planes have opposite spin direction. As can be seen from fig. 1, the signal indeed vanishes for small convergence semi-angles α as expected. However, already for α > 5 mrad, a sizeable EMCD-effect with appropriately alternating sign can be seen. Fortunately, this perfectly matches the region of optimal signal-to-noise ratio [2].

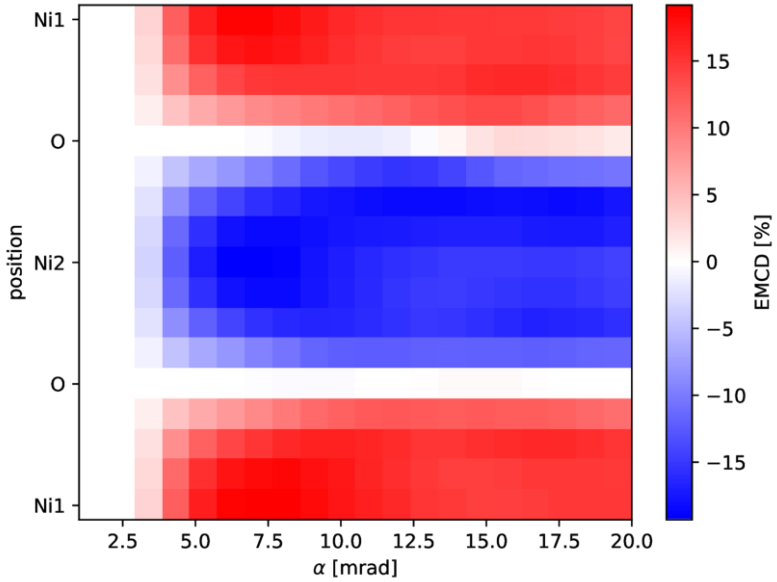

Figure 1. EMCD signal strength as a function of the convergence semi-angle α and the beam position in a 20 nm NiO crystal tilted into systematic row condition including the (1 1 -1) spot. Ni1 refers to spin-up atomic planes, Ni2 refers to spin-down atomic planes. The distance between Ni1 and Ni2 is approx. 0.24 nm. An acceleration voltage of 200 kV and ideal lenses were used in the calculation.

The approach presented here paves the way for the efficient investigation of the magnetic structure of antiferromagnets on the atomic scale. This is not only of interest from a fundamental physics point of view, but can lead to important advances in applications such as spin valves, magnetic sensors, hard disks, or magnetoresistive random-access memory.

References: (Times New Roman, 10-pt, left justified)
[1] P Schattschneider *et al*, Nature **441** (2006), p. 486.
[2] S Löffler and W Hetaba, Microscopy **67** (2018), p. i60.
[3] F Author in “Introduction to abstract writing”, ed. D Writers, (Publisher, City) p.1.

SL acknowledges financial support by the Austrian Science Fund (FWF) under grant nr. I4309-N36.

CCLEM – ZEISS new 3D Multi-Scale Correlative Cryo Light and Electron Microscopy Workflow for Cryo-TEM Lamella Preparation.

Gong-Her Wu[1], Patrick Mitchell[1], Jesus G. Galaz-Montoya[1], Corey W. Hecksel[2], Emily M. Sontag[3], Vimal Gangadharan[4], Jeffrey Marshman[4], David Mankus[5], Margaret E. Bisher[5], Abigail K. R. Lytton-Jean[5], Judith Frydman[3], Kirk Czymmek[6], & Wah Chiu[1,2]

1 Department of Bioengineering, James H. Clark Center, Stanford University, Stanford, CA 94305, USA.
2 Division of CryoEM and Bioimaging, SSRL, SLAC National Accelerator Laboratory, Menlo Park, CA 94025, USA.
3 Department of Biology, James H. Clark Center, Stanford University, Stanford, CA 94305, USA.
4 Zeiss Research Microscopy Solutions, White Plains, NY 10601, USA
5 David H. Koch Institute for Integrative Cancer Research, Massachusetts Institute of Technology, Cambridge, Massachusetts, 02139, USA
6 Advanced Bioimaging Laboratory, Donald Danforth Plant Science Center, Saint Louis, MO 63132, USA

In cryo-TEM lamella preparation, productivity, quality and automation became utmost important. The new Zeiss cryo-correlative workflow allows to determine the volume of interest for TEM lamella preparation by ultra-sensitive cryo-confocal light microscopy. A seamless, well thought through correlative workflow using a uniquely designed sample holder and transfer shuttle is applied to transfer the cryogenic samples to the cryo Crossbeam, as well as the coordinates of the volume of interest for lamella preparation.

The high imaging contrast performance of the ZEISS Cryo-FIB system in mill-and-view mode, enables the operator to cut the lamella exactly at the required subcellular location – in plan-view or cross-section. Furthermore, automation of lamella preparation at several locations economizes the workflow and allows to achieve more high-quality lamellas from a given sample for downstream cryo TEM tomography.

In this work we will present ZEISS unique new correlative cryo light and electron microscopy (CCLEM) workflow and show examples based on the publication “Multi-Scale 3D Cryo-Correlative Microscopy 1 for Vitrified Cells” [1]

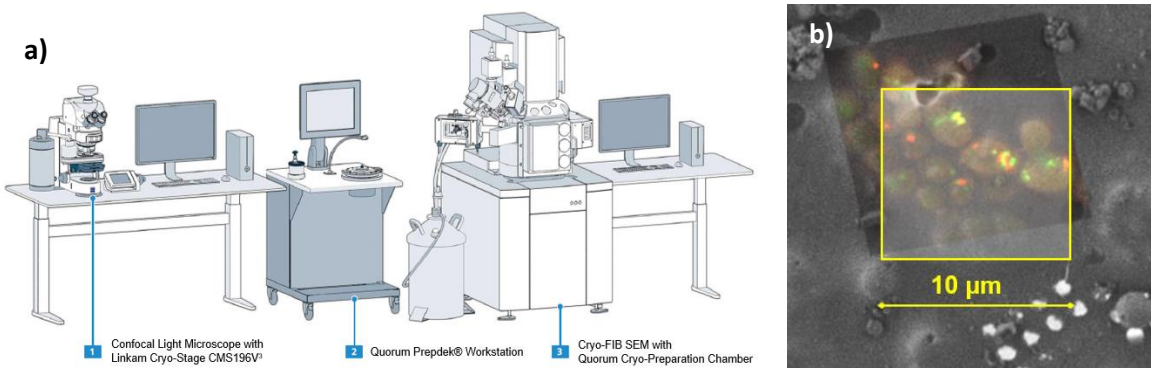

Figure 1. a) Equipment along the new ZEISS Correlative Cryo Light- & Electron Microscopy workflow, **b)** correlative overlap of fluorescence and electron microscopy image of fluorescently-labelled yeast cells.

References:
[1] Wah Chiu *et al*, Structure doi: 10.1016/j.str.2020.07.017

The authors acknowledge the contributions of the Belgrade ELMINA 2018 conference organizers to this guideline by plagiarizing their abstract template in large parts.

Atomic-scale characterization of interface and microstructure of bilayer TaN/TiN thin films on different substrates

Yong Huang, Zhuo Chen, Velislava Terziyska , Christian Mitterer, Zaoli Zhang

Erich Schmid Institute, Austrian Academy of Sciences

Department of Materials Science, Montanuniversität Leoben

TaN/TiN multilayers show great potential among superlattice transition metal nitride systems due to their high hardness and good wear resistance. Meanwhile, this system attracts more interest due to its anomalous hardness variation for various chemical periodicity due to phase transitions of TaNs polymorphs [1]. Different from rock-salt (*rs*) structured TiN_x, which is stable over a wide composition range (0.6<x<1.2) [2], the TaN phase grows in cubic structure due to pseudomorphic stabilization under a critical thickness and then transforms to a hexagonal structure (the ε-TaN structure). Numerous studies suggested that coherency strains and interfaces also play an important role in the hardness enhancement of superlattice systems [1,3–5]. In this work, in order to investigate interface and possible microstructure variations of TaN/TiN, bilayer films composed of TaN and TiN were synthesized by reactive magnetron sputtering on three different substrates. These thin films were characterized by spherical aberration-corrected (Cs-corrected) transmission electron microscopy (TEM, JEOL 2100F). In the film deposited on (100)-oriented MgO substrate, TiN and TaN showed well-grown epitaxial *rs* structure. Detailed high-resolution TEM (HRTEM) studies yielded misfit dislocations with the Burgers vector of a/2<100> and a/2<110>. The maximum spacing between a/2<100> dislocations was measured as about 18 nm, which is well consistent with the theoretical limit for a fully relaxed TaN/TiN (001) thin film. On (0001)-oriented Al_2O_3 substrate, both TiN and TaN were epitaxially grown along (111) orientation. However, numerous twin boundaries were observed in both layers. Polycrystalline and epitaxial columnar grains were observed for the film grown on (100)-oriented Si substrate. These current results will provide great help on further investigations on the growth mechanism of the TaN/TiN system via the epitaxial stabilization and understanding of phase stability in trilayer ε-TaN/*rs*-TaN /TiN superlattices with superior mechanical properties.

The authors kindly acknowledge the financial support by the Austrian Science Fund (FWF): No. **P 33696**. Y.H. also thanks Herwig Felber and Gabriele Felber for help during the sample preparation.

[1] N. Patel, S. Wang, A. Inspektor, P.A. Salvador, Surface and Coatings Technology 254 (2014) 21–27.
[2] TiNx (0.6< x< 1.2): Atomic arrangements, Electronic structure and recent results on crystal growth and physical properties of epitaxial layers, American Institute of Physics, 149 (1986) 95-115.
[3] H. Wang, X. Zhang, A. Gupta, A. Tiwari, J. Narayan, Applied physics letters 83 (2003) 3072–3074.
[4] M. Nordin, F. Ericson, Thin Solid Films 385 (2001) 174–181.
[5] R. Daniel, M. Meindlhumer, J. Zalesak, W. Baumegger, J. Todt, T. Ziegelwanger, J.F. Keckes et al., Materials & Design 196 (2020).

3D Nanoprinting with Electrons - From Meshes to Closed Structures

Anna Weitzer [(1)], Michael Huth [(2)], Gerald Kothleitner [(1,3)] and Harald Plank [(1,3,4)]

(1) Institute of Electron Microscopy and Nanoanalysis, Graz University of Technology, 8010 Graz, Austria

(2) Institute of Physics, Goethe University Frankfurt, 60323 Frankfurt am Main, Germany

(3) Graz Centre for Electron Microscopy, 8010 Graz, Austria

(4) Christian Doppler Laboratory - DEFINE, Graz University of Technology, 8010 Graz, Austria

Additive manufacturing of 3-dimensional objects on the nanoscale is a very demanding task. Among the few capable techniques, 3D nanoprinting via Focused Electron Beam Induced Deposition (3D-FEBID) is a highly promising candidate due to its additive direct-write capabilities with feature sizes below 100 nm on a regular basis and even below 20 nm under optimized conditions. The working principle relies on the localized immobilization of surface adsorbed precursor molecules, injected in the vacuum chamber in gaseous states. Consequently, the demands on substrate materials and in particular surface morphologies are very low, turning 3D-FEBID into a powerful and flexible 3D nanoprinting technology. In the past, however, most fabricated structures were meshed, meaning a combination of differently oriented, individual nanowires, which were connected at specific points in 3D space according to the target application. To leverage this technology to the next level, we here report about the progress to expand 3D-FEBID capabilities from mesh-like towards closed structures.

The main challenge, we had to face is based on local beam heating and its implications on local growth rates. While well understood in meshed structures, closed objects revealed additional dependencies on the dimensions of built objects and the XY pixel position within the structures. Furthermore, electron trajectories are more complex in closed objects, introducing additional proximity effects.

To tackle that problem, we combined finite element simulations with 3D-FEBID experiments and developed a python-based compensation tool, capable of stabilizing the growth in each patterning plane by pre-determined parameter adaptions. The gained insight allowed further expansion, now being applicable for different element-widths and -heights, as demonstrated by more advanced structures. By that, the new model crucially expands FEBID-based 3D nanoprinting by opening up design possibilities for closed and consequently mixed objects for novel applications in various fields of research and development.

Efficient Particles Size Distribution Characterization with TEM: Recent Advances in Experiments and Analysis Automation.

Daniel G. Stroppa[1]

1 Thermo Fisher Scientific, 5651 GG Eindhoven, The Netherlands

Transmission Electron Microscopy (TEM) has been widely used on particles size distribution characterization, particularly with nanostructured samples and in cases that require complementary high-resolution techniques – such as chemical mapping or localized diffraction analysis. Among the numerous applications examples are the quality control on catalysts synthesis and the metallic alloys development by precipitates optimization.

Traditionally, particles size distribution characterization with TEM involves lengthy imaging experiments to support a fair statistical representation of the sample, and extensive image analysis for features identification and measurement. For this reason, TEM is often regarded as an ineffective and expensive approach for the purpose and only recommended in case alternative techniques such as Scanning Electron Microscopy (SEM), X-ray diffraction (XRD) techniques and Dynamic light scattering (DLS) are not applicable.

This presentation features recent instrumentation advances that allow for automated TEM imaging and chemical mapping experiments, and simultaneous data analysis by customizable algorithms for flexible features detection. Results indicates successful unattended TEM imaging experiments and data analysis with high yield (>6000 particles / 10 minutes), and advanced nanoparticles characterization by combining scanning TEM (STEM) imaging, X-rays Energy Dispersive Spectroscopy (EDX) mapping, and Artificial Intelligence (AI) data analysis methods already integrated to an easy-to-use workflow.

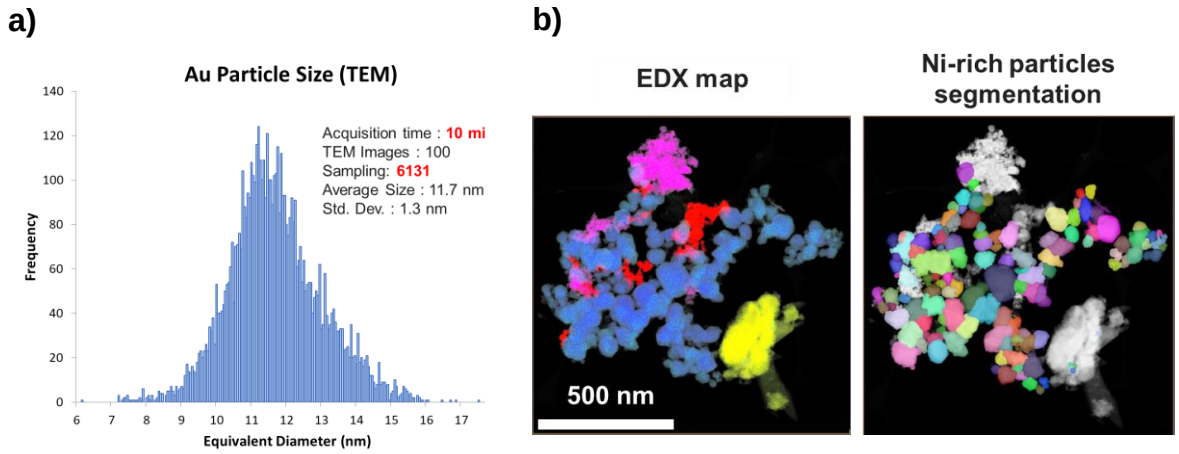

Figure 1. a) Particle size distribution after automated TEM images acquisition and analysis.
b) Experimental EDX mapping result indicating Ni-rich particles (blue) and their automated segmentation for size distribution analysis.

Sub 50nm Transmission Kikuchi Diffraction (TKD) of a TiAlNb TEM lamella using a modern FE-SEM and EBSD system

Roland Schmidt[1], Dominik Zimmer[2], Heike Gabrisch[3]

1 Hitachi High-Tech Europe GmbH
2 Oxford Instruments GmbH NanoAnalysis
3 Helmholtz-Zentrum hereon GmbH

Introduction: The determination of unknown phases and their orientation in crystalline materials can be quite time consuming in a conventional Transmission Electron Microscope (TEM). First, an EDX mapping must be acquired, then the diffraction pattern of representative grains must be found and evaluated manually or by a software support.

Objective: In this presentation a standard TEM lamella was used in a High Resolution Field Emission SEM (Hitachi SU7000) to record simultaneously the EDX and EBSD mappings in Transmission mode (TKD) from a TiAlNb (Ti-42Al-8.5Nb- in at.-%) alloy. Thus, the advantage of a better spatial resolution through a minimized interaction volume by the thin lamella and the speedy access to the profound diffraction library of the EBSD system were combined.

Materials & method: The TiAlNb alloy sample was prepared by hot-isostatic pressing of pre-alloyed powder under 200MPa at 1250°C, standard heat treated and sawed conventionally to a 3mm disc, followed by electropolishing with a solution of perchloric acid in methanol and buthanol at -39°C used for conventional TEM lamella preparation. The method of Transmission Kikuchi Diffraction in the SEM is shortly explained and compared with other diffraction based methods in the SEM, Electron Channeling Contrast Imaging (ECCI) and Electron Channeling Patterning (ECP). The novel concept of the SU7000 is given by the feature that all 6 SEM signals, the Upper SE, the Lower SE, the BSE(Compo), the BSE(Topo), the Middle detector and the CL detector, plus EDX and the EBSD patterns can be recorded at a working distance of 6mm. This allows to use the SEM for High Resolution imaging with in-lens SE at 30kV and at the same time for High Resolution EDX and EBSD, whereas the forward scattered detectors of the EBSD camera act as a kind of "partial" annular dark field (ADF) detector. A high speed EBSD camera (Oxford symmetry, generation1) with a top acquisition speed of 3000 patterns per second and a commercial TKD sample holder were used in the measurements.

Results: The TiAlNb TEM lamella was imaged with the SEM signals, where surface information, such as contamination, were visualized using the Upper SE detector, while the lamella structure of the alloy with less than 44nm lamella spacings was clearly visible in the BSE signal. A 30min simultaneously recorded EDX/EBSD mapping in TKD mode outlines the distribution of a γ-TiAl phase with a $L1_0$structure, space group P 4/m m m, and a hexagonal α_2-Ti_3Al phase, space group P 6_3/m m, with a sub 50nm resolution.

Conclusion: The combination of a Ultra High Resolution Schottky FE-SEM with modern, high speed EBSD systems can be used for a speedy phase analysis of crystals. Even if the sample is prepared for diffraction analysis in the TEM, it may be possible to use it straightforward in the SEM and achieve a lateral EDX/EBSD resolution of less than 50nm.

[1] Gabrisch, H., Lorenz, U., Pyczak, F., Rackel, M., & Stark, A. (2017). Morphology and stability of orthorhombic and hexagonal phases in a lamellar γ-Ti-42Al-8.5Nb alloy-A transmission electron microscopy study. *Acta Materialia*, *135*, 304–313.
[2] Rackel, M. W., Stark, A., Gabrisch, H., Schell, N., Schreyer, A., & Pyczak, F. (2016). Orthorhombic phase formation in a Nb-rich γ-TiAl based alloy – An in situ synchrotron radiation investigation. *Acta Materialia*, *121*, 343–351.

Sample Preparation in Plan-View Geometry for *In Situ* TEM Heating Experiments

N. Šantić[1], A. Minenkov[1] and H. Groiss[1]

Christian Doppler Laboratory for Nanoscale Phase Transformations, Center for Surface and Nanoanalytics, Johannes Kepler University Linz, Altenbergerstr. 69, A-4040 Linz, Austria

Transmission electron microscopy (TEM) plays an important role in the structural analysis of materials. Moreover, *in situ* TEM is rapidly emerging as the premier technique for atomic-scale material characterization in response to external stimuli such as temperature. Heating experiments require the utilization of specially designed sample-holders, nowadays equipped with cutting-edge micro-electro-mechanical system (MEMS) heating chips.[1] Despite all advancements that have been achieved by MEMS-based annealing carriers, studying kinetic processes within the TEM still faces several challenges, including specimen preparation.
It is vital to have a dependable and secure approach that allows obtaining valuable and reliable information from both cross-section and plan-view geometry specimens. In particular, the plan-view geometry is advantageous if kinetic processes of compositional or structural changes should be monitored on free surfaces or, for instance, in thin molecular beam epitaxial (MBE) layers. Being combined with cross-sectional data, a plan-view specimen could facilitate three-dimensional reconstruction of the system's evolution. In general, the plan-view preparation is very challenging [2, 3], especially when the sample is intended for immediate *in situ* TEM inspection. In this case, the specimen preparation must include the devising of thin material slices and their installation on the MEMS-based carrier. During the whole process, the surface of interest must be protected.

We present a step-by-step method to prepare heating chips with plan-view specimens. The preparation protocol starts with the production of wedge-shaped samples in plan-view geometry. The workflow is followed by cutting a plan-view lamella using focused ion beam technique, sample's transfer, and installation on the heating chip (Figure 1) facilitated by the micromanipulator with the rotational axis plug-in. Our approach prevents damage to the surface of interest and has been first tested with MBE-grown Ge quantum dots (QD) on Si. Following the suggested principles, this technique can be adapted to other material systems. The quality of the prepared MEMS chips was validated by scanning electron microscope and TEM. The evaluation will be presented and discussed in detail along with the first heating experiment results.

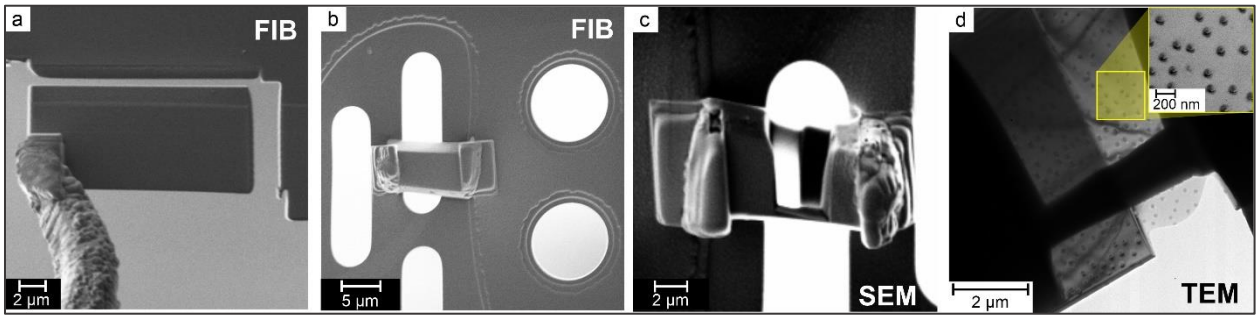

Figure 1. The preparation of the Wildfire MEMS-based heating chip (DENSsolutions): **a)** lift out from the wedge-polished sample; **b)** installation of the lamella on the MEMS heating chip; **c)** final thinning of the sample to electron transparency from the back side; and **d)** validation of the prepared chip with Ge QDs on Si by TEM and SEM.

References:
[1] J.T. van Omme, et al., "Advanced microheater for in situ transmission electron microscopy; enabling unexplored analytical studies and extreme spatial stability", Ultramicroscopy, 192, 2018, p. 14-20.
[2] Li, Chen, et al. "An improved FIB sample preparation technique for site-specific plan-view specimens: A new cutting geometry." *Ultramicroscopy*, 2018, p. 310-317.
[3] Anderson, R., and S. J. Klepeis. "Combined tripod polishing and FIB method for preparing semiconductor plan view specimens." *MRS Online Proceedings Library (OPL)*, 1997, 480.

Towards Damage-Free Molecular Movies with Optical Near-Field Electron Microscopy.

Raphaël Marchand[1,2], Radek Šachl[2], Martin Kalbáč[3], Martin Hof[3], Rudolf Tromp[4,5], Mariana Amaro[3], Sense J. van der Molen[5], and Thomas Juffmann.[1,2]

1 Univ. of Vienna, Faculty of Physics, VCQ, Vienna, Austria.
2 Univ. of Vienna, Max Perutz Laboratories, Dept. of Structural and Computational Biology, Vienna, Austria.
3 J. Heyrovský Institute of Physical Chemistry of the Czech Academy of Sciences, Prague, Czech Republic.
4 IBM T.J. Watson Research Center, New York, USA.
5 Huygens-Kamerlingh Onnes Laboratory, Leiden Institute of Physics, Leiden Univ., Leiden, The Netherlands.

Nanoscale imaging of dynamical processes, occurring in a liquid environment or at interfaces, is of great importance for biomedical applications as well as for materials science and electrochemistry. Yet, the state-of-the-art techniques are currently limited by a trade-off between time and space resolution, by the need of labelling, or by sample damage. Here, we present a label-free imaging scheme, Optical near-Field Electron Microscopy (ONEM) [1], combining damage-free optical excitation of a sample, with an electron microscopy based read-out, potentially offering nanometer resolution at high frame rate, without sample damage, thus allowing for imaging during extended periods.

The principle of ONEM is shown in figure 1 a). The sample (a protein or any nanostructure) is attached to a water-vacuum interface, and is excited with visible light. The resulting near-field interference pattern is converted into a spatially varying electron flux via the photoelectric effect in a few-nanometers thick layer of photocathode material. The experiment takes place in an Aberration-Corrected Low-Energy Electron Microscope (AC-LEEM) [2, 3], allowing for imaging of the photoemitted electrons.

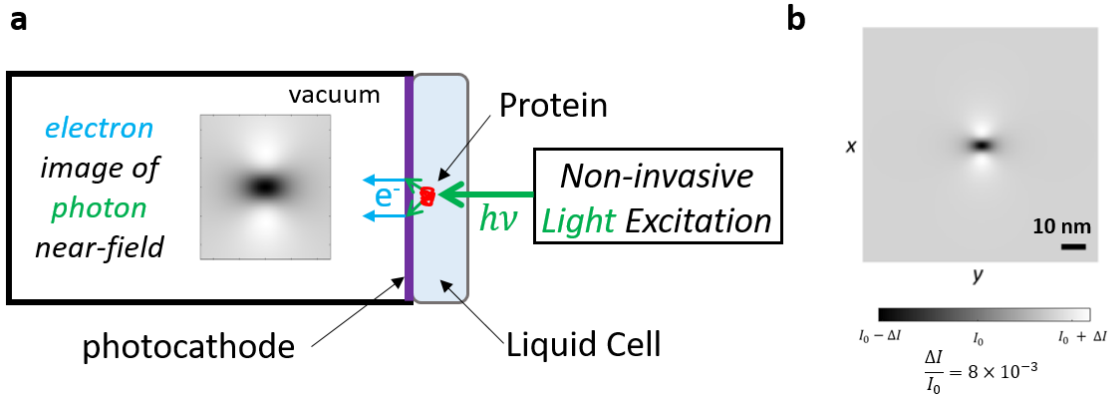

Figure 1. a) Principle of ONEM. **b)** Simulated intensity I(x, y) of the electromagnetic field in the plane of the vacuum-liquid interface for a spherical protein of radius R = 2.5 nm at a distance z = 5nm from the interface. The excitation field is polarized along the x-direction.

Simulations using the MNPBEM toolbox [4] (figure 1b) show that the contrast in the near-(electromagnetic)-field intensity distribution at the photocathode is expected to be of about 1.6 % for a protein of radius R = 2.5 nm, at a distance z = 5 nm from the protein. The simulations also show that the characteristic size of the near-field interference pattern is expected to be of a few nanometers. Given that AC-LEEM has already demonstrated a resolution of a few nanometers, we therefore expect a resolution of a few nanometers for the imaging scheme. We will also discuss why ONEM indeed represents a damage-free imaging technique.

References:
[1] R Marchand, R Šachl, M Kalbáč, M Hof, R Tromp, M Amaro, S. J. van der Molen, and T Juffmann, arXiv:2102.13010 (2021).
[2] R. Tromp, J. Hannon, A. Ellis, W. Wan, A. Berghaus, and O. Schaff, Ultramicroscopy **110/7** (2010), p. 852.
[3] R. Tromp, J. Hannon, W. Wan, A. Berghaus, and O. Schaff, Ultramicroscopy **127** (2013), p. 25.
[4] U. Hohenester and A. Trügler, Computer Physics Communications **183/2** (2012), p. 370.

In situ Transmission Scanning Electron Microscopy as a Tool to Resolve Interface Related Deformation and Fracture in Multilayered Components

Markus Alfreider[1,2,*], Glenn Balbus[2] , Fulin Wang[2], Daniel S. Gianola[2], Daniel Kiener[1]

1 Department Materials Science, Chair of Materials Physics, Montanuniversität Leoben, 8700 Leoben, Austria
2 Materials Department, University of California, Santa Barbara, CA 93106, USA
* markus.alfreider@unileoben.ac.at

With the ongoing miniaturization of components used in day-to-day life, e.g. microelectronics, new processing methods have been developed that are able to produce materials and systems with very confined heterogeneous structures, such as multilayers of only a few tens of nanometres up to micrometres. These structures are often under a non-negligible amount of mechanical load through crystallographic misfits and thermal processing. Thus, from an engineering perspective the question for mechanical parameters with regards to deformation as well as fracture arises. However, as these phenomena are very localized by nature, the large influence of individual constituents makes macroscopic testing techniques rather uninformative. Thus, it is necessary to develop mechanical testing methods at the native scale of such systems, which puts *in situ* testing in electron microscopes into a unique position.

The present work focusses on the interface fracture mechanical investigation in a Si-SiO_x-WTi-Cu multilayer, utilizing *in situ* transmission scanning electron microscopy (TSEM) [1,2], where electron transparent specimens are investigated in a standard 30 kV scanning electron microscope (SEM). In contrast to the more frequently seen scanning transmission electron microscopy (STEM), where the specimen is investigated in a classical 200-300 kV machine, TSEM has two major benefits, when it comes to mechanical investigations. First, the significantly larger space inside an SEM allows for easier mounting of any sort of mechanical testing device and secondly the reduced acceleration voltage allows for stronger defect contrast in the specimen at the drawback of having to produce an even thinner foil. However, with the aid of an adjustable annular STEM detector inside the SEM the same commonly observed imaging modes: bright-field (BF), annular dark-field (ADF) and high angle annular dark-field (HAADF) are obtainable.

Two experiments with different loading configurations (tensile and shear) were conducted showing varying characteristics of ductile failure as well as crack propagation along the WTi-Cu interface. In the light of fracture mechanical concepts and supported analytical and simulation based arguments this gives insight on whether one or the other failing mechanisms is to be expected and leaves a basis for future component design.

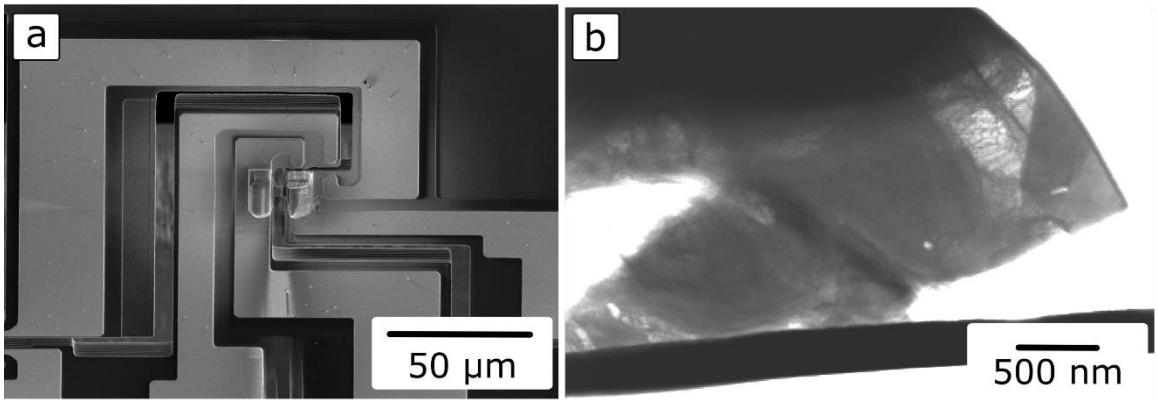

Figure 1. a) Investigated shear specimen on a push-to-pull device before testing. **b)** Final failure of the specimen using TSEM BF imaging

[1] P.G. Callahan *et al.*,Transmission scanning electron microscopy: Defect observations and image simulations, Ultramicroscopy. **186** (2018) 49–61. doi:10.1016/j.ultramic.2017.11.004.

[2] J.C. Stinville *et al.*, Dislocation dynamics in a nickel-based superalloy via in-situ transmission scanning electron microscopy, Acta Mater. **168** (2019) 152–166. doi:10.1016/j.actamat.2018.12.061.

Influence of primary beam energy on localized surface plasmon resonances mapping by STEM-EELS

Michal Horák[1] and Tomáš Šikola[1,2]

1 Central European Institute of Technology, Brno University of Technology, Brno, Czech Republic.
2 Institute of Physical Engineering, Brno University of Technology, Brno, Czech Republic.

STEM-EELS has become a standard technique to map localized surface plasmon resonances (LSPR), which are collective oscillations of free electrons in metal nano- and microstructures. Despite that many works dealing with EELS measurement of LSPR have been published over the last 15 years, there has been no experimental work discussing the experimental conditions during the measurement. Therefore, we have experimentally studied the influence of the primary beam energy and the collection semi-angle on the localized surface plasmon resonances measurement by STEM-EELS to make an instructive overview for the beginners in the field [1].

We took a series of 3 rods and do the STEM-EELS measurement at the primary beam energy of 300 keV, 120 keV, and 60 keV. The best results in terms of the best signal-to-background ratio are obtained using a medium primary beam energy, in our case 120 keV. The primary beam energy should be high enough to suppress the scattering in the sample and at the same time should be low enough to avoid the appearance of relativistic effects. In the case of too high primary beam energy, for example 300 keV, the relativistic effects [2] in the supporting membrane play a non-negligible role and lead to a higher intensity of the background. However, the advantage of the 300 keV electron beam is a lower scattering probability resulting into a better signal to noise ratio in the case of spatial EEL maps of LSPR modes. We note that in the case of a better monochromatization of the primary electron beam (far below 0.1 eV), the elastic part of the background would be significantly reduced which should lead to much better signal to background ratio at lower primary beam energies.

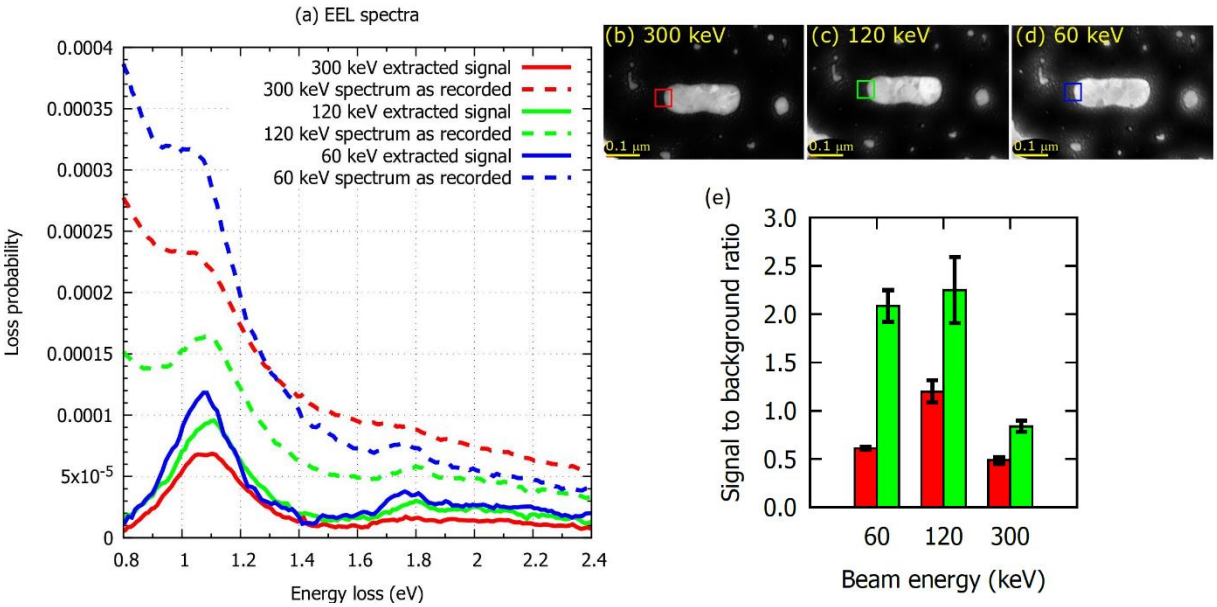

Figure 1. (a) EEL spectra of the same rod at different beam energies; **(b-d)** STEM ADF images of the rod with marked area for integration of the EEL spectra recorded at 300 keV (b), 120 keV (c), and 60 keV (d); **(e)** signal-to-background ratio for the longitudinal dipole (green) and quadrupole mode (red).

References:
[1] M Horák and T Šikola, Ultramicroscopy **216** (2020), p. 113044.
[2] M Horák and M Stöger-Pollach, Ultramicroscopy **157** (2015), p. 73.

Supported by MEYS CR: project CzechNanoLab (LM2018110, 2020-2022). M. H. acknowledges the support of Thermo Fisher Scientific and CSMS scholarship 2019.

Complexion Formation in Solid Oxide Cells - Inter-Diffusion across the Electrode/Electrolyte interface

Franz-Philipp Schmidt[3,4], Hanna Tuerk[1,2], Thomas Götsch[1], Frank Girgsdies[1], Adnan Hammud[1], Danail Ivanov[1], Izaak C. Vinke[5], L.G.J. (Bert) de Haart[5], Rüdiger-A. Eichel[5,6], Karsten Reuter[3,4], Robert Schlögl[1,2], Axel Knop-Gericke[1,2], Christoph Scheurer[3,4], and Thomas Lunkenbein[1]

1 Fritz-Haber-Institut der Max-Planck-Gesellschaft, Department of Inorganic Chemistry, Berlin, Germany
2 MPI for Chemical Energy Conversion, Department of Heterogeneous Reaction, Mülheim/Ruhr, Germany
3 TU München, Department of Chemistry, Garching, Germany
4 Fritz-Haber-Institut der Max-Planck-Gesellschaft, Theory Department, Berlin,Germany
5 Forschungszentrum Jülich GmbH, Institute of Energy and Climate Research, Jülich, Germany
6 RWTH Aachen University, Institute of Physical Chemistry, Aachen, Germany

The intermittent output of renewable energy sources such as wind or solar power requires efficient and long-living technologies to store electrical energy and provide it at later point in time. Solid oxide cells (SOCs) fulfill these criteria, reaching more than 80% efficiency. However, long-term use is not yet feasible predominantly due to degradation, which occurs at the oxygen electrode, therefore limiting the oxygen evolution reaction (OER).

Here we combine state-of-the-art electron microscopy (STEM-EDX, HR-STEM) and theoretical calculations (Monte Carlo, MC) to atomically resolve the interface between the solid electrolyte YSZ (yttria-stabilized zirconia) and LSM ($(La_{0.8}Sr_{0.2})_{0.95}MnO_{3-\delta}$) [1]. In addition, the electronic structure of both materials is analyzed in detail using electron energy-loss (EELS) and X-ray absorption spectroscopy (NEXAFS), as well as density functional theory (DFT). We identified the presence of a significant amount of inter-diffusion between YSZ and LSM, except for strontium, resulting in a shift of 0.8 nm with respect to all other elements. All this is in agreement with MC-based simulations, which includes the ion and site-specific swapping probabilities for the diffusion process. By means of atomically resolved STEM and MC simulations, a reduction of long-range order (partial amorphisation) was observed for a 1.5 nm wide slab on the YSZ side of the boundary, clearly distinguishing it from the bulk fluorite structure.

We identified this slab as a so-called complexion, i.e. a self-limiting interlayer that is stabilized by its confinement between the two adjacent bulk phases, rather than an infinitely sharp interface. These complexions have recently also been discovered in other energy-related systems such as battery materials [2]. The existence of such a finite interlayer provides not only a new perspective to understand the function of SOCs at the atomic scale, it also offers a wide, hitherto unrealized design space.

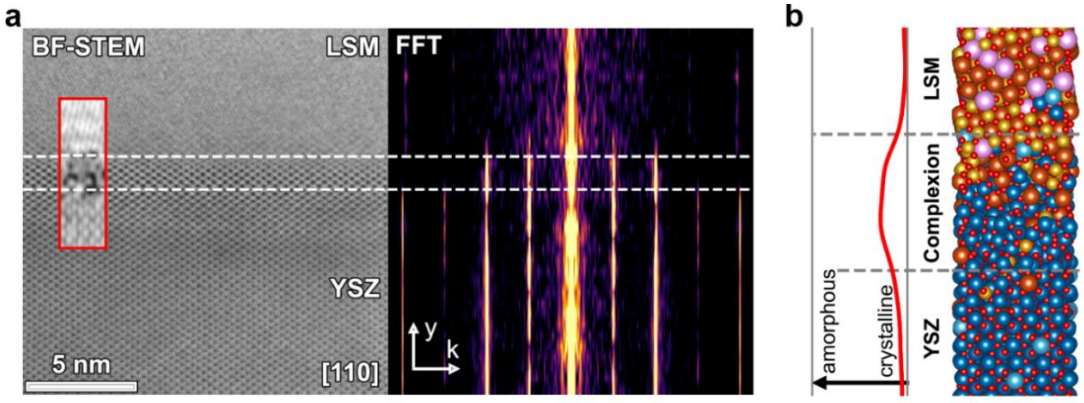

Figure 1. a) Figure 1: (a) BF-STEM image of the YSZ/LSM grain boundary with a superimposed cation density from the MC simulation (inset) in [110] zone axis and semi-reciprocal plot of the micrograph (FFT).The white dashed lines enclose the area of the complexion. (b) MC simulation showing the formation of a complexion.

References:
[1] H. Tuerk, F.-P. Schmidt, T. Götsch et al., submitted

[2] J. Timmermann et al. Phys. Rev. Lett. **125** (2020), 206101

Establishing Organotypic Culture as a Model System to Study the Iron Homeostasis in Human Neurodegenerative Diseases in the Central Nervous System.

Sowmya Sunkara[1], Vanessa Etschmaier[2], Gord Von Campe[3], Silke Patz[2] and Gerd Leitinger[1].

1. Division of Cell Biology, Histology and Embryology, Gottfried Schatz Research Centre, Medical University of Graz, Austria.

2. Research unit for experimental traumatology, University clinic for neurosurgery, Medical University of Graz, Austria.

3. Department of neurosurgery, Medical University of Graz, Austria.

Iron is an essential element in human health and disease. Iron accumulation occurs in neurodegenerative diseases including Alzheimer's disease. Iron deposition in AD is correlated with free radical damage, oxidative stress, amyloid beta plaques (Aβ) and neurofibrillary tangles [1,2]. Though much is known about iron homeostasis in human body, the knowledge of iron homeostasis is very limited in the central nervous system (CNS), especially in pathological conditions like AD. Alzheimer's is well known to affect the cerebral cortex and hippocampus of human brain [3]. However, recent studies report the involvement of spinal cord in AD. Studies report hyper phosphorylation of tau protein and accumulation of Aβ plaques in the spinal cord [3–6]. Currently, research on AD is mostly focused on brain tissue. Other parts of the CNS, including the spinal cord, are less studied in spite of it sharing a similar the cellular content like the brain. Hence, our study is focussed on the effect of Aβ plaques in spinal cord under manipulated iron levels. For this, we opted for an ex-vivo organotypic spinal cord culture as a model system. We initially tested the organotypic culture (OTC) of human brain sections. We observed that the 3D architecture, cell morphology, and neuronal connectivity were well maintained. The immunohistochemical results for the proteins involved in iron homeostasis – Transferrin receptor and ferroportin, confirmed that the cytosolic and membrane proteins are well preserved in OTC. Ferritin was also observed in the tissue, which was observed to be predominantly concentrated in oligodendrocytes and myelin sheath. However, the major con in brain slice cultures is the specimen availability. We observed cancer infiltration in the cultures. Hence, now we opted the human spinal cord for our further studies.

1. Rottkamp, C. A. *et al.*. *Free Radic. Biol. Med.* **30**, 447–450 (2001).

2. Damulina, A. *et al. Radiology* **296**, 619–626 (2020).

3. Uranga, R. M. and Salvador, G. A. *Oxid. Med. Cell. Longev.* **2018**, (2018).

4. Xie, Q., Zhao, W. J., Ou, G. Y. & Xue, W. K. *Brain Sci.* **9**, (2019).

5. Lorenzi, R. M. *et al. Front. Cell. Neurosci.* **14**, (2020).

6. Raudino, F. *Arch. Neurosci.* **3**, (2016).

The authors acknowledge the contributions of Luca Alfred Schmid and Rudolf Schmied. The Austrian Science Foundation FWF funds the project, grant number P 29370, approved by the ethics committee of the Medical University of Graz, number 31-558 ex 18/19.

Expanding Design Possibilities by Blurred Electron Beams during 3D Nanoprinting

Lukas M. Seewald[1], Robert Winkler[1], Gerald Kothleitner[2] and Harald Plank[1,2,3]

1 Christian Doppler Laboratory for Direct-Write Fabrication of 3D Nano-Probes, Institute of Electron Microscopy and Nanoanalysis, Graz University of Technology, 8010 Graz, Austria.
2 Graz Centre for Electron Microscopy, Steyrergasse 17, 8010 Graz, Austria.
3 Institute of Electron Microscopy and Nanoanalysis, Graz University of Technology, 8010 Graz, Austria.

Additive, direct-write manufacturing via focused electron beams has evolved into a reliable 3D nanoprinting technology in recent years [1]. Focused electron beam induced deposition (FEBID) bases on the highly localized immobilization of surface adsorbed precursor molecules by focused electron beams and its subsequent processes. As the precursor is injected in gaseous state, this technology has low demands on substrate materials (vacuum and e-beam compatible) and surface morphology (accessible by the electron beam). By the controlled movement of the electron beam, FEBID allows the fabrication of even complex 3D structures with nanoscale features down to the sub-20 nm range [2,3]. While current trends focus on closed and even bulky 3D designs, most 3D-FEBID structures in the past used meshed objects, meaning a combination of differently oriented branches, connected at some points in 3D space according to the final application. While inherently required for some concepts (e.g. 3D nano-plasmonics [4] or magnetic lattices [5]), the small diameters can also limit final applicability due to low mechanical rigidity, thermal or electric conductivities. To optimize those properties without changing the general 3D design type, a controlled way for tuning individual branch diameters would be highly desirable. Following that motivation, we here introduce on-purpose beam blurring for a controlled upward scaling and study the behaviour at different inclination angles. Aside the intended diameter tunability, the study reveals a massive boost in growth efficiencies up to factor 5 due to strongly changed working regime conditions. As a consequence of the latter, unwanted proximal growth beneath overhanging 3D branches is strongly reduced, which increases the reliability of 3D-FEBID. By that, the study expands the design flexibility of this technology by means of tuneable diameters for meshed objects at higher volume growth rates and reduced proximal growth.

References:
[1] Winkler et al, J. Appl. Phys. **125** (2019) 210901
[2] Frabboni et al, Appl. Phys. Lett. **88** (2006) 213116
[3] Winkler et al, ACS Appl. Nano Mater. **1**, **3**, (2018) 1014-1027
[4] Winkler et al, ACS Appl. Mater. Interfaces **9** (2017) 8233-8240
[5] Keller et al, Sci. Rep. **8** (2018) 6160

High Resolution STEM Simulations of Beryl Crystal Impurities Using Multislice Methods (QSTEM)

Nikola Šimić[1,2], Daniel Knez[2], Ferdinand Hofer[1,2]

1 Graz Centre for Electron Microscopy (ZFE), Graz, Austria
2 Institute of Electron Microscopy and Nanoanalysis, Graz University of Technology, Graz, Austria.

The development of Scanning Transmission Electron Microscopy (STEM) has enabled measuring and analyzing many kinds of materials with atomic resolution. Not only does high resolution imaging give us the opportunity to intuitively interpret crystal structures, but it also enables us to find local crystal defects and impurities. This is especially useful in the analysis of a beryl crystal $Al_2Be_3[Si_6O_{18}]$, where empty channels exist due to the crystal structure. STEM investigations with a high-angle annular dark field detector (HAADF) of a beryl crystal parallel to the hexagonal c-axis reveal all structural details, even the empty channels between the atom columns (Figure 1a). However, some channels do not appear to be empty. This could mean that we see dopant elements, long known from literature, localized in the channels of naturally grown beryl [1,2]. In order to prove that the contrast detected is not an artefact, a multitude of multislice simulations was performed using various detector and microscope settings in the program QSTEM [3]. Several alkaline ions such as Na, K and Cs were placed inside the empty channels of a crystal model with varying thicknesses, with the atoms being chosen according to EDS and WDS spectral analysis of the beryl performed in a scanning electron microscope.

The simulation results show that the contrast of dopant atoms matches that from STEM HAADF measurements. This work proposes methods for the identification of channel atoms and shows their feasibility as well as a wide range of possibilities for improvement of identification quality. Methods of differentiating between stacks of light atoms and singular heavy atoms are proposed as well.

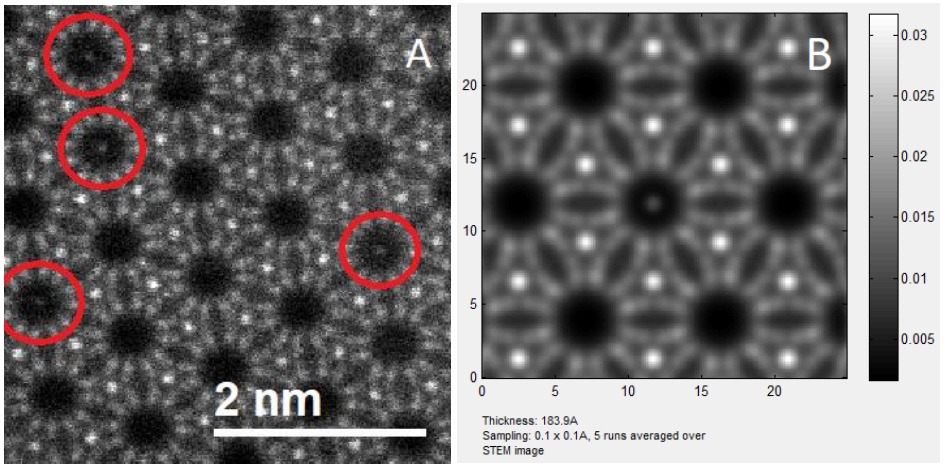

Figure 1. a) STEM image of beryl recorded with a HAADF detector (ASTEM investigation by C. Gspan in February 2015) **b)** STEM simulation of beryl with a thickness of 18 nm. A single Cs atom was placed inside the center channel at the first atomic layer in z-direction.

Acknowledgements: We thank Sanja Šimić and Stefan Mitsche for the SEM-EDS-WDS analyses.

References:
[1] C. Gspan, F. Hofer, FELMI-ZFE Performance Report 2012-2014, Graz University of Technology, 2015.
[2] V. Arivazhagan, F.D. Schmitz, P.E. Vullum, A.T.J. van Helvoort, B. Holst, J. Microscopy, 265 (2017) 245.
[3] C. T. Koch in "Determination of core structure periodicity and point defect density along dislocations", PhD thesis, Arizona State University, 2002.

Multimodal & Multiscale materials characterization in battery research: the game changer Xe plasma FIB-SEM

Tom Jäpel[1], Dean J. Miller[2] and Jiří Dluhoš[3]

1 TESCAN Gmbh, FIB-SEM Application material science, Dortmund, Germany.
2 TESCAN USA Inc., principal scientist, Warrendale, PA, USA.
3 TESCAN ORSAY Holding a.s., Product manager FIB-SEM material science, Brno, Czech Republic.

Ga-FIB-SEMs are widely used and very powerful analytical instruments, because they can provide a lot of information from materials microstructures. However, there are some limitations. Among those are the limited scale and throughput; the dimensions of which we can analyze using a Gallium based FIB. Researchers may find situations where they like to analyze a larger cross section or larger volume than can be easily or even possibly prepared using a Ga-FIB. Thus there is a need to expand that capability for larger scale. A second issue with Ga-based FIB is gallium contamination: gallium is a metal so it can react with various materials leading to changes in the microstructure or affecting the properties of materials that are going to be prepared with FIB-SEM, which then are possibly subjected to subsequent testing. A third area of challenge is amorphization and damage. Amorphization or damage is intrinsic to the sputtering process with an ion beam. The ion will displace atoms. The atoms that are near surface may be sputtered away but some of these displaced atoms will remain in the sample. If those don't return to their equilibrium position, we introduce defects and ultimately even amorphization in the sample and that can compromise the quality of samples for a variety of measurements.
Xe-Plasma FIB-SEMs mitigated or eliminated some of those limitations for Ga based FIBs and expanded even further the opportunities of these powerful instruments for materials characterisation.
This talk is going to be about how we can use these instruments in a powerful way for multimodal and multiscale materials characterisation on the example of Lithium ion battery research.

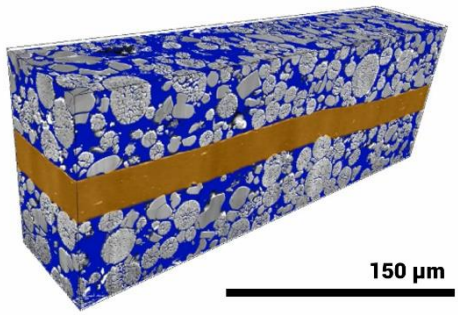

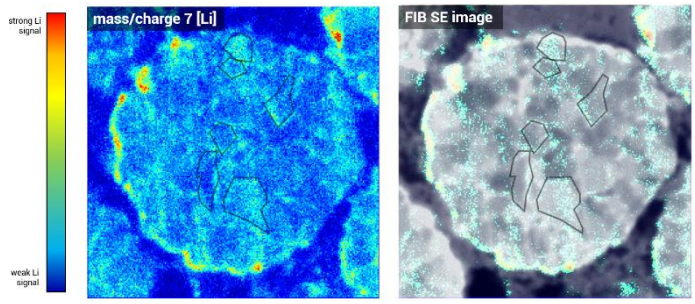

Figure 1 (left). 3D Xe-Plasma FIB-SEM large scale/multiscale tomography reconstruction and segmentation of a Lithium-ion battery cathode foil.
Figure 2 (right). Xe-Plasma FIB-SEM prepared cross section, multimodal imaged with an integrated ToF-SIMS of a battery primary particle. The ToF Analysis of the Li ion content after cycling reveals an increased amount on grain boundaries [1].

References:
[1] T. Sui, B.Song, Jiri Dluhos et al. Nano Energy, 17, 254-260 (2015)

"Flash and Freeze" in Brain Slices: Structure-Function Analysis of Synapses in the Central Nervous System by Electron Microscopy

Carolina Borges-Merjane[1], Olena Kim[1], Peter Jonas[1]

1 Institute of Science and Technology (IST) Austria, Cellular Neuroscience, Klosterneuburg, Austria.

Historical attempts to develop methods to bridge how synaptic physiology and synaptic ultrastructure are related date back to the middle of the 20th century [1, 2, 3]. The goal of such approaches is to obtain millisecond-time precision with nanometer-space resolution to capture rapid ultrastructural changes during synaptic transmission. These include the seminal experiments that proved the vesicular hypothesis with freeze slamming at the frog neuromuscular junction [3, 4]. However, applying similar approaches to mammalian central synapses remained difficult.

In a recent attempt to address structural changes during synaptic transmission, optogenetic stimulation was combined with cryo-fixation by high-pressure freezing (HPF) and subsequent electron microscopy, through a method termed "flash and freeze" [5, 6]. In this technique, a light pulse activates genetically expressed channelrhodopsin (ChR2) in presynaptic neurons, leading to action potential initiation and vesicle fusion at the active zone of the presynaptic terminal. The sample is frozen by HPF at precisely defined time intervals after the onset of the stimulation, allowing to capture the structural changes underlying synaptic transmission. Although the method was successfully applied to the worm *C. elegans* [5] and dissociated hippocampal neuronal cultures [6], whether it could be used to study thicker brain tissue sections remained unknown.

Our work used an enhanced Flash and Freeze method, with the Leica EM ICE with Light Stimulation system to assess mechanisms underlying synaptic transmission at an identified cortical synapse, the mossy fiber-to-CA3 pyramidal cell synapse in mouse hippocampus, during basal transmission and after short-term plasticity. For the first time, we applied this functional electron microscopy method to acute brain slices and organotypic slice culture, for detailed ultrastructural analysis of synapses in an intact network environment [7]. Our results show release of vesicles after single and multiple stimuli, with depletion of the docked-vesicle pool at active zones as a structural correlated to the functionally measured readily-releasable pool of vesicles, as well as ultrafast endocytosis.

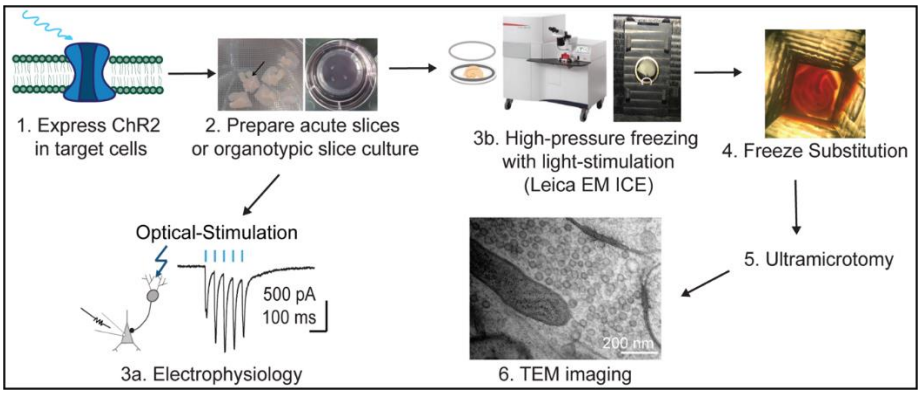

Figure 1: Flash and Freeze workflow diagram

References:
[1] MH Ellisman *et al*, Journal of Cell Biology **68** (1976) 752-774
[2] JE Heuser and TS Reese, Journal of Cell Biology **57** (1973) 315-344
[3] JE Heuser *et al*, Journal of Cell Biology **81** (1979) 275-300
[4] JE Heuser and TS Reese, Journal of Cell Biology **88** (1981) 564-580
[5] S Watanabe *et al*, Elife **2**:e00723 (2013)
[6] S Watanabe *et al*, Nature **504** (2013) 242-247
[7] C Borges-Merjane, O Kim and P Jonas, Neuron **105** (2020) 992-1006
We thank our funding sources: C.B.M MSCA H2020 708497 and FWF V 739-B27; PJ (OK) FWF W1205-B09; PJ ERC 692692 and FWF Wittgenstein Z 312-B27.

In-situ TEM Investigation of Toughening in Silicon at Small Scales

Inas Issa[1], Christoph Gammer[2], Stefan Kolitsch[2,3], Anton Hohenwarter[1], Peter J. Imrich[1], Reinhard Pippan[2], Daniel Kiener[1]

[1] Department Materials Science, Chair of Materials Physics, Montanuniversität Leoben, Jahnstrasse 12, A-8700, Austria.
[2] Erich Schmid Institute of Materials Science, Austrian Academy of Sciences, Jahnstrasse 12, A-8700 Leoben, Austria.
[3] Materials Center Leoben Forschung GmbH, Roseggerstrasse 12, A-8700 Leoben, Austria.

Highly brittle materials such as Silicon (Si) commonly experience instable fracture at room temperature (RT) due to high Peierls stresses of their crystal lattice. However, it is well known that materials reach higher strength at small scale, and this may eventually impact the brittle ductile transition (BDT) and toughening, even for highly brittle materials. Fundamentally, reaching sufficiently high stresses to nucleate and move dislocations from an atomistic stress concentrator prior to fracture would generate a shielding effect that provides some toughening contribution [1]. Knowledge concerning the possibility to shift the BDT temperature of Si to RT solely by geometric reduction to the sub-micron scale is still lacking. Herein, we explore the size range [90-350] nm via quantitative in-situ TEM fracture experiments on pre-notched single crystal (SC) Si bending beams in conjunction with advanced in-situ nanoscale strain mapping [2] and detailed FEM simulations.

Machining of bending beams is carried out using FIB. *In-situ* TEM fracture experiments are performed using a Picoindenter PI-95 from Hysitron, Inc.. *In-situ* TEM strain mapping using nano diffraction strain mapping around the crack tip, as it allows measuring local transient strain fields during loading. Therefore, a series of diffraction patterns was recorded in STEM mode using a 2 nm step size.

Our findings consist a brittle bulk fracture behavior of large samples at a stress intensity K_{IC}~1 MPa.$m^{1/2}$. However, below characteristic dimensions of about 250 nm, the fracture toughness strikingly increases inversely with size to at least triple. TEM observations show that below this critical transition length, nucleation and propagation of dislocations occur, shielding the crack tip and enabling the unprecedented rise in fracture toughness, see **Figure 1 a).** Advanced *in-situ* TEM strain mapping reveals the stresses at the crack tip approach the theoretical strength in small specimens. FEM calculated elastic strain map of a computational digital twin with identical dimensions loaded to the same shows excellent agreement and validating the plane strain condition and respective data analysis, **Figure1 b).**

In conclusion, we were able to measure the complex strain field in front of the crack tip during *in-situ* TEM fracture experiments on SC Si nanobending beams. Below characteristic dimensions of about 250 nm, the fracture toughness strikingly increases inversely with size to at least triple.

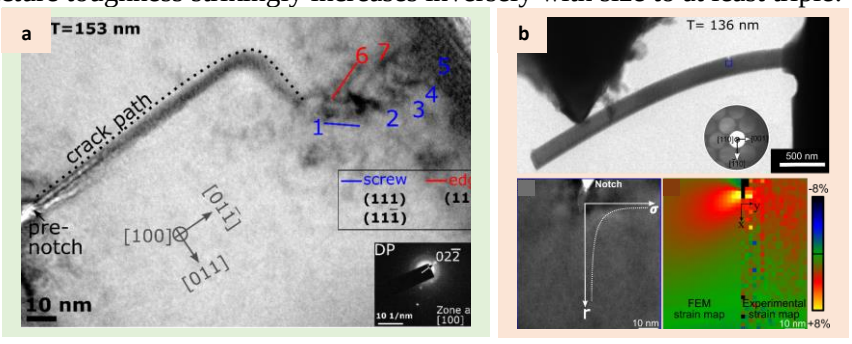

Figure 1. a) FIB thinned post mortem BF TEM image of a crack tip trapped by few dislocations acquired under **g**(02$\bar{2}$). **b)** *In-situ* strain mapping during a nanoscale fracture experiment on SC Si.

References:

[1] Cleri, F. *et al.* Atomic-Scale Mechanism of Crack-Tip Plasticity: Dislocation Nucleation and Crack-Tip Shielding. Phys. Rev. Lett. **79**, (1997), p.1309–1312.
[2] Gammer, C. *et al*. Local and transient nanoscale strain mapping during in situ deformation. Appl.Phys.Lett. (2016), **109.**

Imaging the Spatial Distribution Of π^* States In Graphene

M. Ederer[1,*], M. Bugnet[2,3,4], V. Lazarov[5], Q. M. Ramasse[2,3], D. M. Kepaptsoglou[2,5], and S. Löffler[1]

[1] TU Wien (Austria), [2] SciTech Daresbury Campus (UK), [3] University of Leeds (UK), [4] Université de Lyon (France), [5] University of York (UK), [*] manuel.ederer@tuwien.ac.at

Electronic states are responsible for most macroscopic properties of materials, ranging from electrical and magnetic to optical properties. Only recently has it been shown that directly mapping the electronic orbitals of bulk samples in real space is possible [1]. In this work, we present π^*/σ^* orbital maps of multi-layered graphene, acquired via transmission electron microscopy and electron energy loss spectroscopy, and demonstrate the excellent agreement between simulations and experiment. Specifically, the channeling of the incident electron beam can modify the localization of the EELS signal, and thus greatly complexify the interpretation of energy-filtered atomic-resolution state maps.

Orbital mapping is based on using only electrons from a small energy-loss window for the image generation. Thus, only the transition to a single final electronic state, in this case a π^* or σ^* orbital of graphene, is visible. As a sample, we use multiple quasi free-standing layers of graphene, epitaxially grown on 6H-SiC. The accompanying simulations are based on the multislice method and the mixed dynamic form factor approach [2], calculated from density functional theory simulations [3]. The resulting maps show, surprisingly for both orbitals, an intensity maximum at the atomic columns. With simulations for samples with different thicknesses we could pinpoint this result to elastic channelling effects that emerge as soon as the sample is a few unit cells thick. The different spatial distributions of the orbitals become much more apparent for the ratio between the π^* and σ^* orbital maps, as then the channeling effect is at least partly cancelled. Fig. 1 shows clearly that the π^* orbitals extend further in between the atomic columns. The profiles in Fig. 1(c) display this even more pronounced, the maximum of the ratio profile is located exactly between the atomic columns, indicated by the maximum of the HAADF profile.

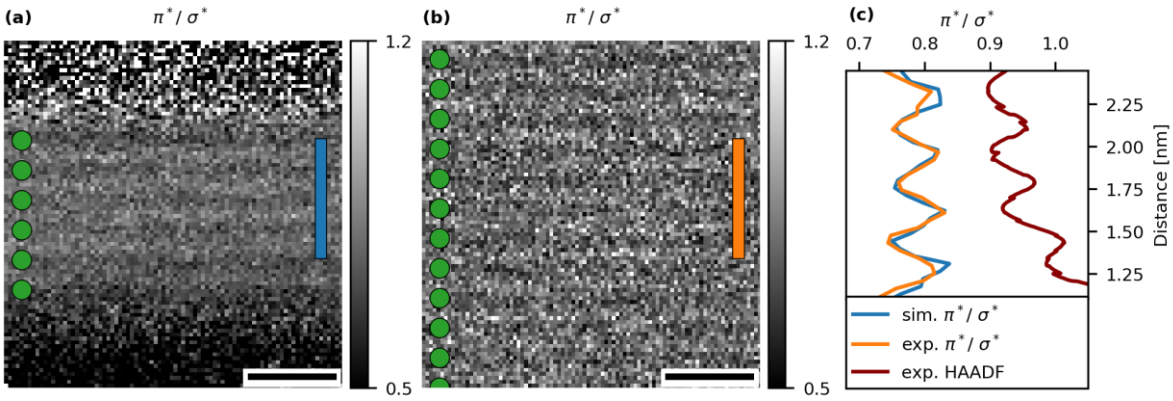

Fig. 1. Ratio of π^* to σ^* orbital maps. The graphene layers (marked by green disks) are oriented in the [2 1 3 0] zone axis. The specimen thickness is approximately 25 nm and the acceleration voltage 60 kV. The scalebars indicate 0.5 nm. **(a)** Experimental map. **(b)** Simulated map with shot noise. **(c)** π^*/σ^* profiles from (a) and (b), integrated in the range indicated by the blue and orange bars, together with the experimental HAADF signal.

The excellent agreement between the simulations and the experiments shows the potential of orbital mapping and opens up the way for broad applicability on interfaces and crystal defects in the future.

References:
[1] Löffler et al., Ultramicroscopy, **26** (2017), p. 177.
[2] Löffler et al., Ultramicroscopy, **39** (2013), p. 131.
[3] Blaha et al., The Journal of Chemical Physics, **152** (2020), p. 074101.
The authors gratefully acknowledge funding from the Austrian Science Fund (FWF) under grant nr. I4309-N36. Experiments were performed at the SuperSTEM Laboratory (UK) with support from the Engineering and Physical Science Research Council (EPSRC).

Relationship of Microstructure and Magnetic Domain Configuration of a Spinodally Decomposed $Cu_{52}Ni_{34}Fe_{14}$ Alloy.

Thomas Radlinger[1], Ferdinand Hofer[1,2] and Gerald Kothleitner[1,2]

1 Institute of Electron Microscopy and Nanoanalysis, Graz University of Technology, Steyrergasse 17, 8010 Graz, Austria
2 Graz Centre for Electron Microscopy, Steyrergasse 17, 8010 Graz, Austria

Various alloys have shown to be promising materials in terms of manipulating magnetic properties by controlling their microstructure. Despite extensive research activities on such nano-scale magnetic materials for several decades now, the relationship between the evolution of the microstructure and its magnetic properties still remains to be fully explored. [1–4]. In this study, we investigate a spinodally decomposed CuNiFe alloy, using a wide variety of modern (S)TEM methods such as dark-field imaging, EDX spectroscopy and differential phase contrast (DPC) imaging. The specimen under investigation was solution treated and a subsequent heat treatment at 625°C for 10 hours leads to a spinodal decomposition of the alloy [3,5]. EDX elemental maps reveal the characteristic stripe/plate like Ni-rich phase embedded in a Cu-rich matrix [1,2]. Those plates are growing along the [100] directions of the crystal which is shown in figure 1 a). The EDX analysis reveals a chemical composition of 54 at% Ni, 27 at% Fe and 19 at% Cu for the Ni-rich phase which, is similar to the findings of Kobayashi et al [4]. To investigate the magnetic structure, LM-STEM DPC with a switched off objective lens was performed to ensure a nearly field-free environment. In DPC, the deflection of the electron beam due to the interaction with the magnetic field of the specimen is measured with a 4-quadrant annular detector. An in-plane magnetic induction map is shown in figure 1 b), in which the colour represents a certain direction of the magnetic field. The induction map displays a complicated pattern of 90° and 180° domains. Furthermore, these domains exhibit in-plane field vectors not parallel to the [100] directions. Therefore, the DPC findings suggest other directions, such as [111], to be the magnetic easy ones.

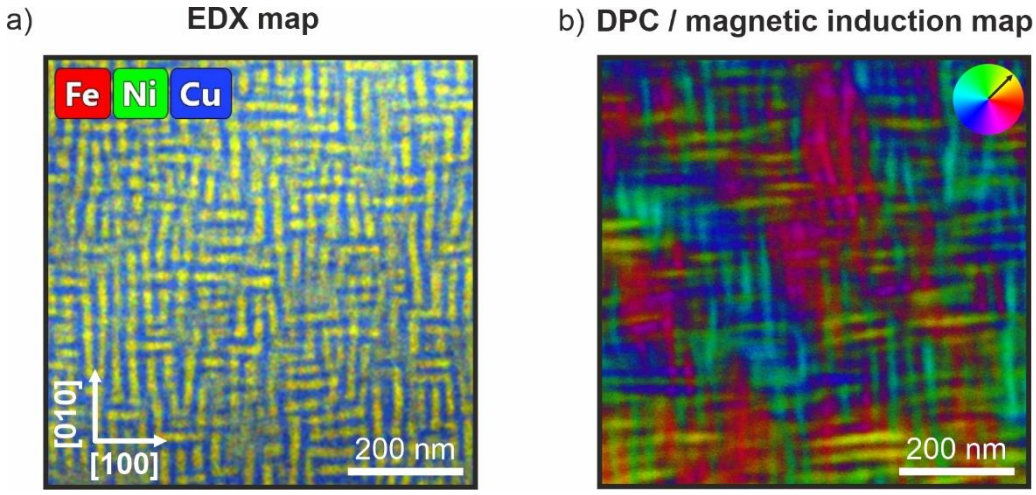

Figure 1: a) Color coded EDX elemental map along [001] zone-axis orientation using Ni K, Cu K and Fe K signals. Ni-rich plates (yellow) are embedded in a Cu-rich matrix (blue). b) Magnetic field map from 4-quadrant DPC signal. The colour of a certain position represents the direction the magnetic field is pointing. The colour-wheel relates to the direction of the field.

References:
[1] E P. Butler, G Thomas, Acta Metallurgica **18** (1970), p. 347-365.
[2] H Li, X Hao, G Zhao, S Hao, Journal of Materials Science **36** (2001), p. 779–84.
[3] S Kang et al, Met. Mater. Int. **18** (2012), p. 521–525.
[4] S Kobayashi et al, Molecules **25** (2020), p.3282.
[5] J-S Kim, M Takeda, D-S Bae, Jpn. J. Appl. Phys. **55** (2016), p.123002.

The JSM-IT800 series - The next level of Intelligence Technology in FE-SEM combining ultrahigh resolution and unprecedented ease of use.

Georg Raggl[1]

[1]JEOL (Germany) GmbH; Gute Änger 30; D-85356 Freising; Germany

JEOL is a world leading manufacturer of electron- and ion-optical systems. The company's portfolio includes lithography tools using both electron and ion beams as well as characterization systems like Scanning Electron Microscopes (SEM) and Transmission Electron Microscopes (TEM).
Advances in materials and life sciences necessitate an increasing performance of the imaging and analytical capabilities of modern Field Emission Scanning Electron Microscopy (FE-SEM) systems. The new JSM-IT800 FE-SEM series is a highly stable yet flexible platform to encounter a variety of applications ranging from morphological and chemical studies to the crystallographic analysis of a wide variety of materials. In addition to the brand new easy to use "SEM Center" user interface, the high-performance electron emitter ensures a fast and easy sample characterization.

The JSM-IT800 series comes with a patented JEOL In-Lens Schottky Plus Field Emission Electron Gun, a state of the art electron optical control system called „Neo Engine" and a JEOL EDS system which is fully integrated into the „SEM Center" user interface. The In-Lens Schottky Plus Emitter allows the user to conduct high resolution imaging, high speed elemental mapping and EBSD and Soft X-ray analysis by providing high probe currents at low accelerating voltages (e.g. 100 nA @ 5 kV). The systems ease of use is acomplished by JEOL`s new electron optical engine (Neo Engine) providing both, stable observation conditions and enhanced auto-functions. In addition, the JSM-IT800 series offers two objective lens types to satisfy the individual user requirements. The Hybrid Lens (HL) system is tailored for general purpose applications whereas the Super Hybrid Lens (SHL) version is used for observation and analysis at ultra low accelerating voltages at highest resolution. Moreover, the JSM-IT800SHL introduces the Upper Hybrid Detector (UHD) as the newly integrated standard In-Lens detector of the system which enables the user to obtain images with significantly enhanced Signal to Noise ratio allowing for an easy observation with high image fidelity.

Besides the standard Everhart-Thornley and UHD detector, a variety of new backscatter electron detectors can be incorporated into the JSM-IT800 systems. The Scintillator Backscattered Electron Detector (SBED) enables material contrast imaging at low accelerating voltages due to its excellent sensetivity whereas the multi-segment Versatile Backscatter Electron Detector (VBED) allows for additional 3D-topographical imaging.

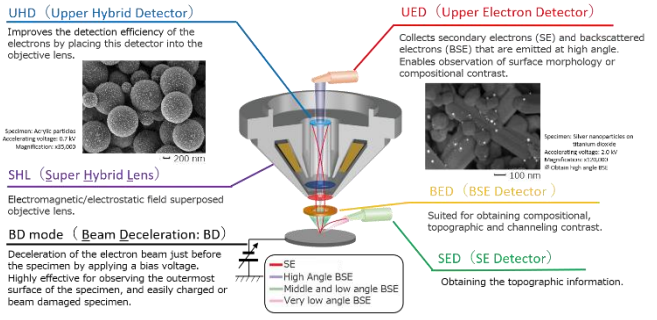

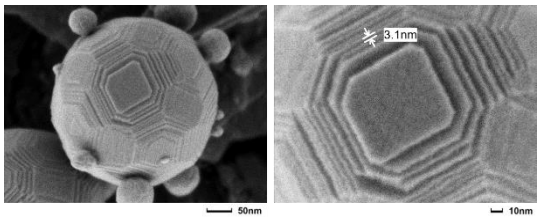

Figure 1 (left). Schematic of the detector setup of the JSM-IT800SHL Field Emission Scanning Electron Microscope. **Figure 2 (right).** High resolution images of alumina particles acquired @ 500 V acceleration voltage using JEOL`s new Upper Hybrid Detector.

MEMS-based *in situ* Electron-Microscopy Investigation of Rapid Solidification and Heat Treatment on Eutectic Al-Cu [1]

Phillip Dumitraschkewitz[1], Matheus A. Tunes[1], Diego Santa Rosa Coradini[1], Thomas M. Kremmer[1], Parthiban Ramasamy[2], Peter J. Uggowitzer[1] and Stefan Pogatscher[1]

[1]Chair of Nonferrous Metallurgy, Department of Metallurgy, Montanuniversitaet Leoben, Franz-Josef-Str. 18, 8700, Leoben, Austria
[2]Erich Schmid Institute of Materials Science, Austrian Academy of Sciences, Jahnstraße 12, A 8700 Leoben, Austria

The solidification behavior of a eutectic AlCu specimen is investigated via in situ scanning transmission electron microscope (STEM) experiments. Solidification conditions are varied by imposing various cooling rates via a micro-electro-mechanical system (MEMS) based membrane. The methodology allows the use of material processed by a melting and casting route close to industrial metallurgically fabricated material for in situ STEM solidification studies. Several rapid solidification morphologies could be obtained solely on a single specimen by the demonstrated strategy. A change from nanometer scaled lamellar to dendritic morphology is observed by differing cooling from medium to the highest tested rates. Cooling rates of 100, 10000 and 30000 K/s are used. For the comparatively slow cooling rate of 100 K/s, a coarser three-dimensional morphology is gained. Additional post-solidification heat treatments are investigated in terms of observation of spheroidization of lamellas during annealing at elevated temperatures. [1]

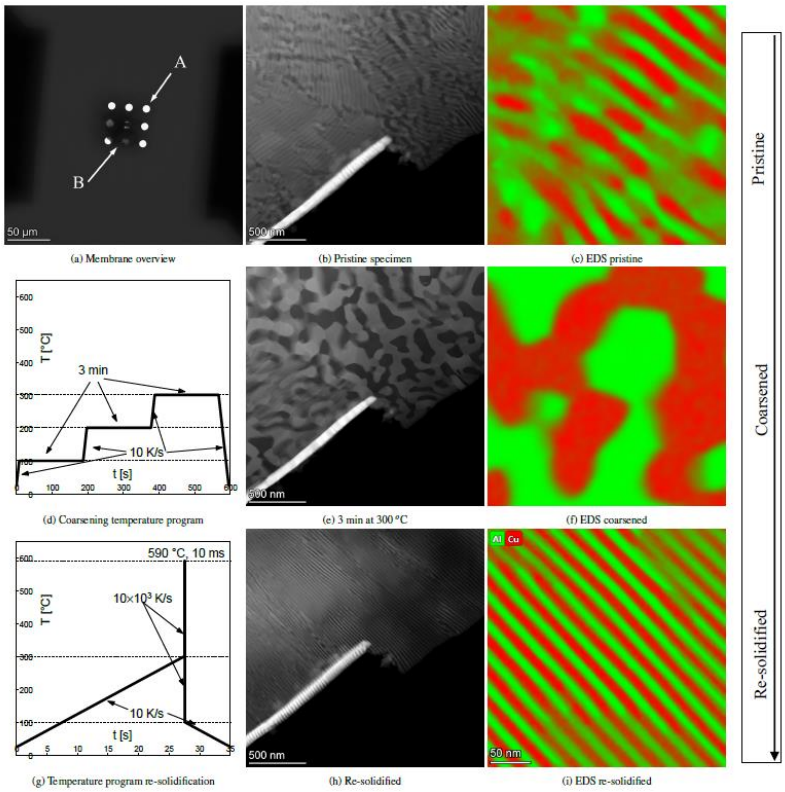

Figure 1. Overview of the membrane, HAADF and EDS images of the pristine, coarsened pristine and re-solidifed material with corresponding temperature programs. **a)** Membrane overview with membrane holes (feature A) and specimen (feature B). Following microstructures are obtained: **b,c)** lamellar colonies with varying orientation; **e,f)** interconnected spheroidized grains; **h,i)** unidirectional lamellas. Bright areas in HAADF show the θ-Al_2Cu and dark areas are α-Al phase as identified by EDS. **h,i)** After re-solidification a newly formed nanostructured hierachy is obtained, consisting of α -Al and θ-Al_2Cu unidirectional lamellas. The bright feature, reaching approximately into the center of the figure **b,e,h)**, is a roll-up of the sample. [1]

References:
[1] Dumitraschkewitz *et al*, arXiv:2101.02935v1 (2021)

In situ TEM Study of Sn-Ge Nanosystem Thermal Stability

Alexey Minenkov, Heiko Groiss

Christian Doppler Laboratory for Nanoscale Phase Transformations, Center for Surface and Nanoanalytics, Johannes Kepler University Linz, Altenbergerstr. 69, A-4040 Linz, Austria

One of the main objectives of modern scientific advancement is to address the need for efficient nanomaterials with advanced properties, which could be tuned in a controlled fashion. Ge-Sn alloy is utterly perspective by virtue of adjustable bandgap, and compatibility with current Si-based technology [1]. Pursuant to recent findings, the Sn concentration in the alloy, which assures indirect-to-direct bandgap transition should be more than 6,5 at.%. This value significantly exceeds the known bulk equilibrium solubility of Sn in Ge, which makes the desired alloys drastically nonequilibrium. The large lattice mismatch between components and the smaller surface energy of Sn govern the Sn segregation to the surface at relatively low temperatures. This process severely alters the sample crystallinity and rules out the efficient material applications, thus must be avoided. Sad but true, our comprehension of the Sn-Ge alloy thermal stability is still scarce, especially, at the nanoscale.

At that point, *in situ* TEM heating could bring more light to advanced material characterization allowing real-time observation and identification of the specimen phase state. Our previous investigations in the field, testify the utilization of layered films formed in a high vacuum via PVD as a suitable model system for complex interphase interaction studies. These objects provide clean atomic contact between components that is crucial for their interactions research. Additionally, the initial a-Ge state allows us to study the metal-induced crystallization process (MIC) at the nanoscale. Experiments were conducted in Jeol JEM-2200FS TEM (HRTEM, SAED, HAADF, STEM EDX) equipped with an in-column Ω-filter, a TVIPS TemCam-XF416 CMOS-based camera and fitted with the MEMS-based Wildfire heating holder from DENSsolutions.

The thoroughly traced morphological and structural evolution of Ge-Sn nanofilms is documented with video sequences. Conjunction of specimens with a characteristic size of 25 nm inspected in plan-view and cross-sectional geometries (Figure 1) gives us the ground to propose the stages of the interphase interactions at heat-treatment [2]. The components' interdiffusion process is activated at approximately 90°C leading to homogenization of the system. The MIC process governs the formation of diamond structured Ge-Sn solid solution through self-assembly. At rising temperatures, Sn segregation to the surface takes place at ≈150°C followed by the melting of the Sn-rich phase in the 150-190°C range. The established temperatures of phase transitions, as well as the achievable, stable Sn concentration, are size-dependant and should be considered for the successful synthesis and application of nanosized Ge-Sn alloys with an enhanced Sn content.

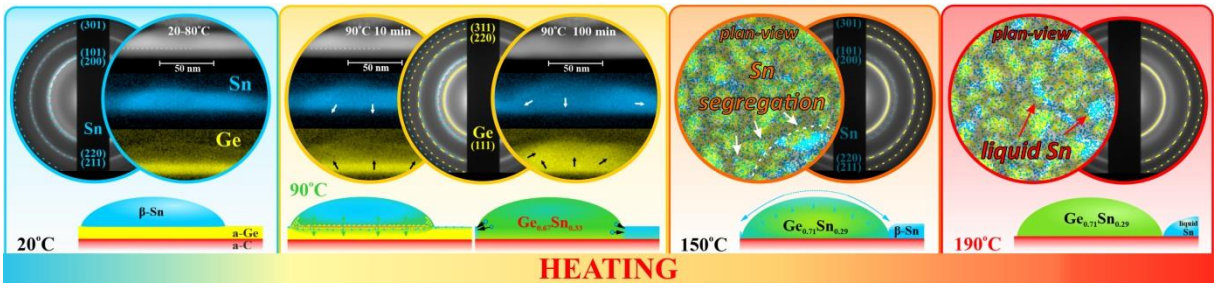

Figure 1. The interphase interactions in Sn/Ge film at heat-treatment.

References:
[1] J Doherty et al., Chem. Mater. **32, 11** (2020) p. 4383.
[2] A Minenkov, H Groiss, J. Alloys Compd. **859** (2021) 157763.

The authors gratefully acknowledge the financial support from the Austrian Federal Ministry for Digital and Economic Affairs, the National Foundation for Research, Technology and Development and the Christian Doppler Research Association.

High Pressure Freezing and Glycan Microarray Analysis Indicate High Resistance of Green Algal *Mougeotia* and *Spirogyra* Zygospores

Charlotte Permann[1], Ancuela Andosch[2], Klaus Herburger[3], Andreas Holzinger[1]

1 Department of Botany, University of Innsbruck, Functional Plant Biology, 6020 Innsbruck, Austria
2 Department of Biosciences, University of Salzburg, 5020 Salzburg, Austria
3 Department of Plant and Environmental Sciences, University of Copenhagen, 1871 Frederiksberg, Denmark

Streptophytic green algae include the closest living relatives to land plants. Zygnematophyceae have been proposed as the immediate sister lineage to embryophytes and only recently published genomes will allow new insights into terrestrialization. Zygnematophyceae perform a special type of sexual reproduction in the form of conjugation. In the present study, we have investigated this process in more detail, because zygospores resulting from sexual reproduction are likely a key adaptation to non-aquatic habitats. We studied the conjugation morphology (Fig. 1 a) and the zygospores of two different genera, *Spirogyra* (Fig. 1 a-e) and *Mougeotia* (Fig. 1 f-i), collected in the Austrian Alps. One *Spirogyra* species and two *Mougeotia* species were determined by the surface structure of the zygospore wall. The three different layers of mature zygospore walls were investigated after chemical fixation or high-pressure freeze fixation. We found a polysaccharide rich exo- and endospore, which showed a distinct orientation of the microfibrils in *Spirogyra* (Fig. 1 d, e) but were smooth in *Mougeotia* (Fig. 1i). However, both genera had a distinct electron dense mesospore, composed of lipid- and sporopollenin-like substances (Fig. 1d, e, i). The chemical composition of the cell wall layers was confirmed by confocal RAMAN spectroscopy, allowing to detect polysaccharides in the exo- and endospore and a lipid- and aromate-rich layer in the mesospore. Glycan microarray analysis of both genera revealed the occurrence of pectins (homogalacturonan (HG)), hemicelluloses (xyloglucans/ xylans), extensins and arabinogalactan proteins (AGPs) in the cell walls. In conclusion, our results suggest a reorganization of the zygospore wall during maturation, leading to a highly resistant and protective structure that helps algae to tolerate harsh environmental conditions.

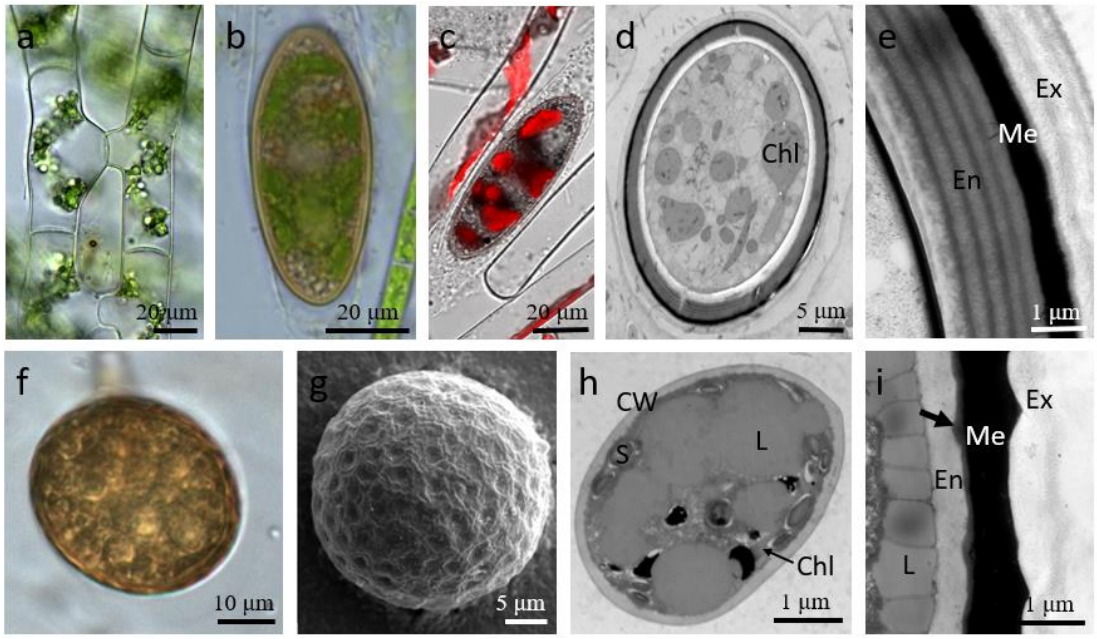

Figure 1. **Conjugation and zygospores of Zygnematophyceae from field samples collected at Kühtai, Tyrol, Austria. a-e)** *Spirogyra sp.*. **f-i)** *Mougeotia sp.*. **a)** conjugating stage. **b)** mature zygospore. **c)** CLSM micrograph. **d)** TEM micrograph. **e)** TEM micrograph, mature zygospore wall. **f)** mature zygospore. **g)** SEM micrograph. **h)** TEM micrograph, young zygospore with single layered cell wall. **i)** TEM micrograph, mature zygospore wall (arrow indicates a lipid-like fourth layer). **Abbreviations** Chl chloroplast, CW cell wall, En endospore, Ex exospore, L lipid bodies, Me mesospore, S starch grain.

The Impact of High-Tension on the Orbital Mapping of Rutile by STEM-EELS

Michael Oberaigner[1], Daniel Knez[1], Stefan Löffler[2], Gerald Kothleitner[1,3]

1 Institute of Electron Microscopy and Nanoanalysis, Graz University of Technology, Graz, Austria
2 University Service Centre for Transmission Electron Microscopy, TU Wien, Wien, Austria
3 Graz Centre for Electron Microscopy, Graz, Austria

Recently, it was shown that scanning transmission electron microscopy (STEM) in combination with electron energy loss spectroscopy (EELS) allows for a real-space mapping of atomic orbitals of rutile at 80 kV [1]. The major challenge of such experiments is the inherently poor signal-to-noise ratio (SNR). We propose a reliable post processing path for mapping orbitals and demonstrate the mapping of orbitals for rutile at different operation voltages.

Due to the different bond lengths between titanium and oxygen, rutile exhibits orbitals which are rotated 90° to each other when viewed along the [001]-direction (Figure 1a). The specimen is prepared by wedge polishing and focused ion milling. The measurements are performed with a FEI Titan³ G2 equipped with a monochromator and Cs-corrector. The EELS signal is recorded by a K2 (Gatan) direct detection camera, which offers higher SNR through its much-improved detective quantum efficiency.

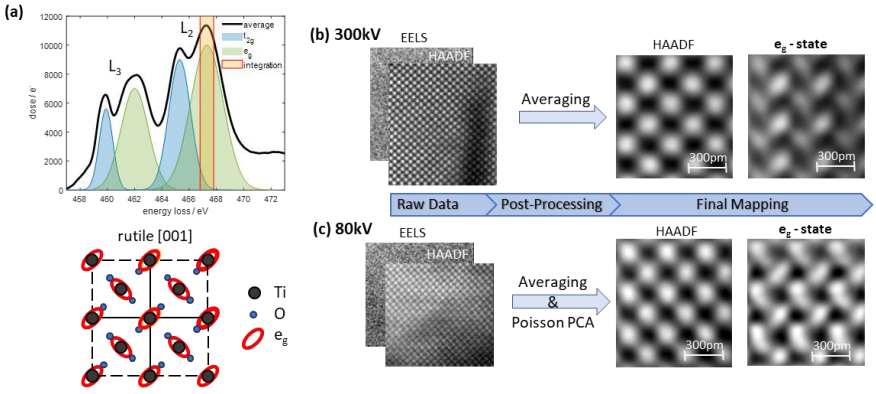

Figure 1. a) EELS signal at $L_{2,3}$-edges of titanium in rutile with the contribution of each state. The marked energy range is used to map the e_g-states, which are rotated 90° to each other in rutile [001]. **b)** and **c)** Orbital mapping of rutile at 300 kV and 80 kV.

Although using direct electron detection, mapping orbitals from the raw spectrum images requires extra processing even after a principle component analysis (PCA) denoising step. Therefore, the SNR ratio is first increased by precisely stacking and re-aligning multiple cells by reference to a simultaneously acquired dark field image. The corresponding EELS spectrum is averaged and can be further denoised by PCA. The noise of a direct detection camera is mostly governed by the shot noise contribution, which enables the application of weighted PCA optimized for such Poisson noise dominated data [2].
Figure1 b and c show the results of such a mapping sequence. At higher operation voltages, a sufficiently high SNR is already achieved with averaging the EELS signal, so that PCA denoising is not necessary. Nevertheless, at lower voltages no beam damage is observed and the orbital features appear larger. These effects will be discussed.

[1] S. Löffler et al, Ultramicroscopy, 177 (2017), pp. 26–29
[2] M. R. Keenan and P. G. Kotula, In Surf. Interface Anal., 36 (3) (2004), pp. 203–21

The authors acknowledge financial support by the Austrian Science Fund (FWF) under grant nr. I4309-N36 and by the Zukunftsfonds Land Steiermark Project: “ASTEM Upgrade”

Reconstructing Parent Microstructures from EBSD based Orientation Measurements

René de Kloe[1], Stuart Wright[2]

1 EDAX, Ringbaan Noord 103, 5046AA Tilburg, The Netherlands
2 EDAX LLC, 91 McKee Drive, Mahwah, NJ, 07430, USA

When a material undergoes a transformation from one crystallographic phase to another, a grain in the original microstructure may transform into several different crystallographic variants. The transformed microstructure is generally quite different but often traces of the original microstructure are recognizable. For example, in steels, austenite (face-centred cubic γ) is formed during high temperature processing and then transforms to ferrite (body-centred cubic α) as it cools to room temperature. It is difficult, if not impossible, to capture the microstructure of the high-temperature phase. It would be helpful to be able to characterize the microstructure (i.e., grain size, texture) of the high-temperature phase to optimize the full processing path of the material.

We have implemented the method by Ranger et al. [1] in conjunction with EBSD to allow reconstruction of the original high-temperature microstructures in a range of materials. The efficacy of the method was verified in cobalt (figure 1), steel, and titanium (figure 2) samples using in-situ heating, comparison with alternative models, and retained grains of the high temperature phase.

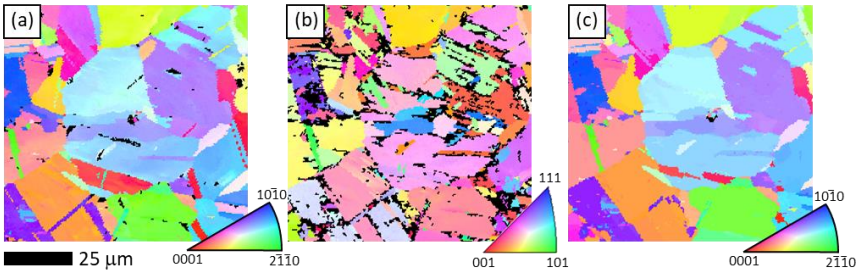

Figure 1. Cobalt parent grain reconstruction as verified by in-situ heating experiment **a)** Observed high temperature β-Co microstructure by in-situ heating **b)** Observed α-Co microstructure after cooling **c)** Reconstructed β-Co based on room temperature microstructure

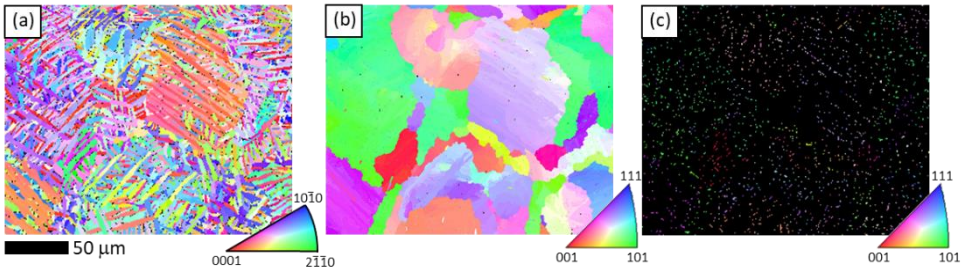

Figure 2. Titanium parent grain reconstruction as verified by retained β-Ti grains **a)** α-Ti structure as observed, **b)** reconstructed microstructure **c)** retained β-Ti grains

Because local misorientations between adjacent pixels instead of entire grains are used to identify the phase relationships, also orientation gradients like those displayed within several of the grains in Figure 2(b) may be present in the reconstruction and can provide an indication of residual strain in the material prior to the phase transformation.

The parent grain reconstruction algorithm performs well and allows quantitative aspects of the pre-transformation microstructure such as grain size, crystallographic texture, and even residual strain to be reliably characterized.

Reference:
[1] C. Ranger *et al.*, Metall. Mater. Trans. A 49 (2018) pp 4521-4535

In-situ Nanoscale Characterization of Electrical and Magnetic properties of 3D Nanostructures by combination of AFM, SEM and FIB

C.H. Schwalb[1], J. Hütner[1,2], R. Winkler[3], P. Frank[2], M. Wolff[1,2], and H. Plank[3]
[1]*Quantum Design Microscopy GmbH, Darmstadt, Germany*
[2]*GETec Microscopy GmbH, Vienna, Austria*
[3]*Institute for Electron Microscopy and Nanoanalysis, Graz Univ. Technology, Graz, Austria*

Combining different analytical methods into one instrument is of great importance for the simultaneous acquisition of complementary information. Especially the in-situ combination of scanning electron microscopy (SEM) and atomic force microscopy (AFM) enables completely new insights in the micro and nano-world. In this work, we present the unique in-situ combination of scanning electron and ion microscopy (SEM/FIB) and atomic force microscopy (AFM) for nanoscale characterization [1-3].

We will present a variety of case studies to highlight the advantages of interactive correlative in-situ nanoscale characterization for different materials and nanostructures. We show results for *in-situ* electrical characterization by conductive AFM for 2D materials (Figure 1) as well as electrostatic force microscopy (EFM) of piezoceramic films.

In a further step, we demonstrate how in-situ correlative analysis with the AFSEM in an SEM can be extended into the third dimension to measure nanomechanical properties of soft material. To achieve this, FIB slicing and mapping of nanomechanical properties using the AFSEM is performed in repetitive steps to build up a 3-dimensional elasticity map.

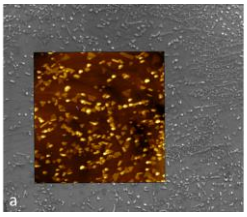

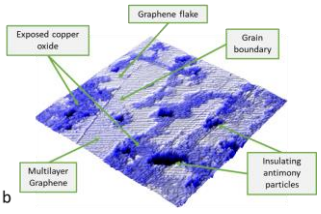

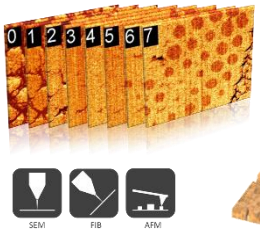

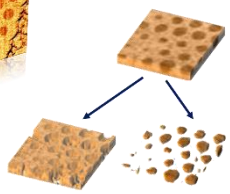

Figure 1 (left). Conductive AFM measurements done using AFSEM® nano a) Correlative SEM and AFM image of on Cu/Graphene/Antimony sample. b) 3D topography overlaid with conductivity signal showing distinct regions. (Light regions correspond to high current and dark regions correspond to low current). **Figure 2 (right).** (Left) 3D subtractive tomography measurements of ion-beam sliced polymer samples with encapsulated beads. The reconstructed 3D elasticity map (Right) clearly reveals the harder beads inside the softer polymer.

In addition, we will present first results for the in-situ characterization of magnetic nanostructures by combination of SEM and high-vacuum magnetic force microscopy (MFM). SEM enables to identify grain boundaries in, e.g., duplex steel samples, where the magnetic properties at the grain boundaries can be directly analyzed via MFM to characterize the magnetic properties with nanometer resolution and distinguish between ferromagnetic and paramagnetic domains.

Based on the broad variety of applications regarding the nanoscale characterization of different materials and devices we anticipate that correlative analysis by combination of in-situ AFM and SEM/FIB will be one of the driving characterization tools in the future.

References:
[1] D. Yablon *et al.*, Microscopy and Analysis **31(2)** 14-18 (2017)
[2] J. Kreith *et al.*, Rev. Sci. Instr. **88** 053704 (2017)
[3] S.H. Andany *et al.*, Beilstein J. Nanotechnol. **11**, 1272-1279 (2020)

In-situ atomic-resolution observation of coherent twin boundary migration in CrN

Zhuo Chen [(1)], Zaoli Zhang[1)]

1 *Erich Schmid Institute of Materials Science*
of the Austrian Academy of Sciences, Jahnstrasse 12 ,8700 ,Leoben ,Austria

It is well known that most crystal structures do not possess simple geometric arrangements, which determines their more complex deformation mechanism. For complex material deformation, Kronberg proposed a synchronous slip and twinning deformation mechanism in 1957, whereby two shears operate in opposite directions on adjacent atomic planes [1]. This mechanism has been shown to operate in the Laves phase and α-Alumina [2, 3]. However, due to the difficulty of characterization of complex materials, there has been no *in-situ* experimental evidence to support this deformation mechanism for many years. In this work [4], using *in-situ* atomic-resolution electron microscopy, we report two different twin boundary defect (TD) nucleation and CTB migration modes at the CTB/ITB (incoherent twin boundary) and CTB/surface junctions. A new twin defect nucleation and CTB migration mode are observed from the CTB/surface junction. We show that such CTB migration is associated with a boundary structure alternating from an N-terminated to Cr-terminated, involving Cr and N atom respective motion, i.e., asynchronous CTB migration (as seen in Fig.1). We further reveal the dynamic and thermodynamic mechanism of such asynchronous migration through strain analysis and DFT simulations. Our findings uncover an atomic-scale dynamic process of defect nucleation and CTB migration in a binary system, which provides new insight into the atomic-scale deformation mechanism in complex materials.

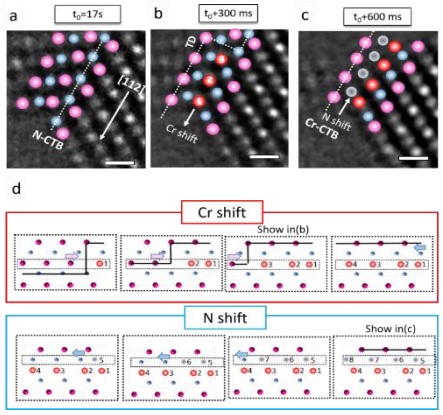

Fig. 1. **(a)-(c)** HRTEM images (snapshots of Movie) of the initial state, transitional state, and final stage of CTB migration from N-terminated to Cr-terminated, respectively. **(d)** Schematic sequence of asynchronous CTB migration and the TD movement.

Reference:

[1] M.L. Kronberg, Plastic deformation of single crystals of sapphire: Basal slip and twinning, Acta Metallurgica 5(9) (1957) 507-524.
[2] M.F. Chisholm, S. Kumar, P. Hazzledine, Dislocations in Complex Materials, Science 307(5710) (2005) 701-703.
[3] N. Shibata, M.F. Chisholm, A. Nakamura, S.J. Pennycook, T. Yamamoto, Y. Ikuhara, Nonstoichiometric Dislocation Cores in α-Alumina, Science 316(5821) (2007) 82-85.
[4] Z. Chen, Y. Zheng, L. Löfler, M. Bartosik, H. Sheng, C. Gammer, D. Holec, Z. Zhang, Real-time atomic-resolution observation of coherent twin boundary migration in CrN, Acta Materialia, Volume 208, 2021, 116732.

Acknowledgements:

The financial support from the China Scholarship Council (CSC, 201608120053) for one of the authors, Z.C., is acknowledged. The authors thank *Dr. Matthias Bartosik and Prof. Paul H. Mayrhofer* for the thin film synthesis at TU Wien for the sample preparation. *Lukas Löfler and Dr. David Holec* are gratefully acknowledged for DFT calculation.

Advancements in segmentation of 3D SEM images of neurons: pre-processing steps

Snježana Radulović[1], Lucie Chalet[2], Benjamin Gottschalk[3], Stefan Wernitznig[1], Armin Zankel[4] and Gerd Leitinger[1]

[1] Gottfried Schatz Research Center, Division of Cell Biology Histology and Embryology, Medical University Graz, Austria; [2] University of Franche Comté, Besançon, France; [3]Gottfried Schatz Research Center, Division of Molecular Biology and Biochemistry, Medical University Graz, Austria; [4] Institute of Electron Microscopy and Nanoanalysis, NAWI Graz, Graz University of Technology and Graz Centre for Electron Microscopy, Austria

Reconstructing neurons from serial EM micrographs and localizing synapses manually is extremely time consuming [1][2]. Advanced, semi-automatic selection tools for segmenting are faster, but require noise reduction while keeping membrane integrity and structural features of synapses. We developed pre-processing steps to make the micrographs suitable for semi-automatic selection.

Serial electron micrographs of identified neurons of the locust, *Locusta* migratoria were produced using serial block face scanning electron microscopy (Fig. 1A). Several image processing steps were performed sequentially on these stacks, using ImageJ software.

First, a histogram matching algorithm was used to homogenize brightness levels, followed by a low pass Fourier transform band-filter to isolate small structures like cell-membranes, a rolling ball algorithm to give the cell membranes a higher contrast, and an automated Otsu threshold. The thresholded stacks were analyzed with the particle analyzer to filter out small irregular components. In parallel, the particle analyzer was used once more with settings that enabled keeping the large particles such as mitochondria. The result was subtracted from the result of the first round with the particle analyzer.

Second, mitochondria were removed, for this, the histogram - matched stacks were filtered with a median filter after a contrasting step, followed by a Huang´s auto threshold to get a binary image (that contained the mitochondria) which was subtracted from the first preprocessing step.

The first step successfully removed noise and small structures, but mitochondria attached to the membranes were still visible, compromising the results of segmenting (Fig. 1B).

During the second preprocessing step most of the structures inside the cells were deleted. However, at certain locations the membranes appeared discontinuous. Nevertheless combining both steps with fast selection tools significantly enhanced segmentation efficiency compared to a traditional manual approach. (Fig. 1C)

In summary, pre-processing can improve the accuracy and efficiency of segmenting algorithms.

Fig. 1 A: Original micrograph B. result of first pre-processing step. C. result of second pre-processing step

[1] Seeing what is coming: building collision-sensitive neurones. Rind FC, Simmons PJ. Trends Neurosci. 1999 May;22(5):215-20. Review.

[2] Role of an identified looming-sensitive neuron in triggering a flying locust's escape. Santer RD, Rind FC, Stafford R, Simmons PJ. J Neurophysiol. 2006 Jun;95(6):3391-400.

[3] Optimizing the 3D-reconstruction technique for serial block-face scanning electron microscopy. Wernitznig S, Sele M, Urschler M, Zankel A, Pölt P, Rind FC, Leitinger G. J Neurosci Methods. 2016 May 1;264:16-24

Supported by the Austrian Science Fund FWF (P 32058 and P 32376 to GL and SW).

Implications of Low Substrate Temperatures on Growth Dynamics during 3D Nanoprinting via Electrons

Jakob Hinum-Wagner (1), Robert Winkler (1), David Kuhness (1), Gerhard Birnstingl (2), Gerald Kothleitner (2), and Harald Plank(1,2,3)

1 Christian Doppler Laboratory - DEFINE, Graz University of Technology, 8010 Graz, Austria
2 Institute of Electron Microscopy and Nanoanalysis, Graz University of Technology, 8010 Graz, Austria
3 Graz Centre for Electron Microscopy, 8010 Graz, Austria

As the need for reliable 3D-printing at the nanoscale is rapidly increasing, appropriate methods have to be developed to push their capabilities beyond former limitations. In the small pool of capable techniques, Focused Electron Beam Induced Deposition (FEBID) is a promising candidate, as it enables the mask-less, direct-write fabrication of freestanding 3D nano-architectures with a high flexibility concerning design, material and functionality. This technology relies on the local decomposition of surface adsorbed precursor molecules by a focused electron beam. The local precursor coverages crucially determine incremental growth rates and thus predictability, precision and reliability. Recently, it was found that local heating by the electron beam itself can impact the precursors residence time at the growth front, which changes the effective coverage up to a point, where further growth becomes unstable [1]. Based on those insights, we here turn around the situation and lower the substrate temperature to study the implications on growth stability and fabrication precision. We use 3D multi-pod designs and study growth dynamics (growth rates), morphological peculiarities (structural dimensions, branch bending), for a temperature range of 5 °C to 30 °C. In a second step, we vary the leg numbers of the multi-pods and demonstrate the implications on growth rates. We found a boost in vertical growth up to a factor of 2.4- and 5.6-times higher vertical and volume growth rates for 5 °C compared to 25 °C. Results also show temperature-independent wire curvatures, and that the shape fidelity of multipod architectures is maintained at substrate temperatures down to 5 °C. However the growth history plays an important role during fabrication at different temperatures, which is demonstrated by the investigation of the growth behaviour of single pillars atop the multipod structures. These findings demonstrate the applicability of this low substrate temperatures approach for 3D-FEBID, leading to reduced process times without further drawbacks.

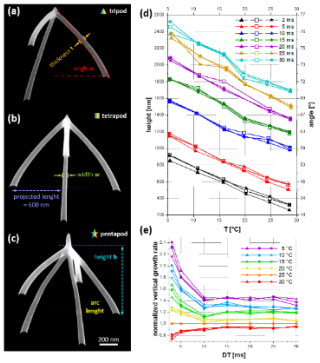

Figure 1: *(a)-(c): SEM images of multipod geometries, fabricated at 5 keV, 28 pA, a dwell time of 3 ms and a substrate temperature of 5 °C including measurement procedures. (d): measured heights h as a function of the substrate temperature for multipods (indicated as triangles, rectangles and stars, respectively) fabricated with different dwell times and (e) vertical growth rates normalized to the growth rate of multipod fabricated at a substrate temperature of 25 °C.*

References:
[1] Mutunga et al., ACS Nano (2019).

Fusion of mitochondria to 3-D networks, autophagy and increased organelle contacts are important subcellular hallmarks during cold stress in plants

Philip Steiner[1,2], Othmar Buchner[2], Ancuela Andosch[2], Gerhard Wanner[3], Gilbert Neuner[4] and Ursula Lütz-Meindl[2]

1 Present affiliation: Institute of Pharmacology, Medical Faculty, Johannes Kepler University, Linz, Austria
2 Department of Biosciences, Paris Lodron University, Salzburg, Austria
3 Department Biology I, Ludwig-Maximilians University, Munich, Germany
4 Department of Botany, Functional Plant Biology, Leopold Franzens University, Innsbruck, Austria

Low temperature stress has severe impact on distribution, physiology and survival of plants in their natural habitats [1,2]. While numerous studies have focused on physiological [3] and molecular adjustments [4] to low temperatures, this study provides evidence that cold induced physiological responses coincide with distinct ultrastructural alterations. Three plants from different evolutionary levels and habitats were investigated: The freshwater alga *Micrasterias denticulata*, the aquatic plant *Lemna* sp. and the nival plant *Ranunculus glacialis*. Ultrastructural alterations during low temperature stress were determined by employment of 2-D transmission electron microscopy and 3-D reconstructions from focused ion beam – scanning electron microscopic series. With decreasing temperatures, increasing numbers of organelle contacts (Fig. 1a) and particularly fusion of mitochondria to local networks (Fig. 1a,b) were observed. We assume that the increase or at least maintenance of respiration during low temperature stress is likely to be based on these mitochondrial interconnections. Moreover, it is shown that autophagy and degeneration processes accompany freezing stress in *Lemna* (Fig. 1c) and *R. glacialis*. This might be an essential mechanism to recycle damaged cytoplasmic constituents to maintain the cellular metabolism during freezing stress.

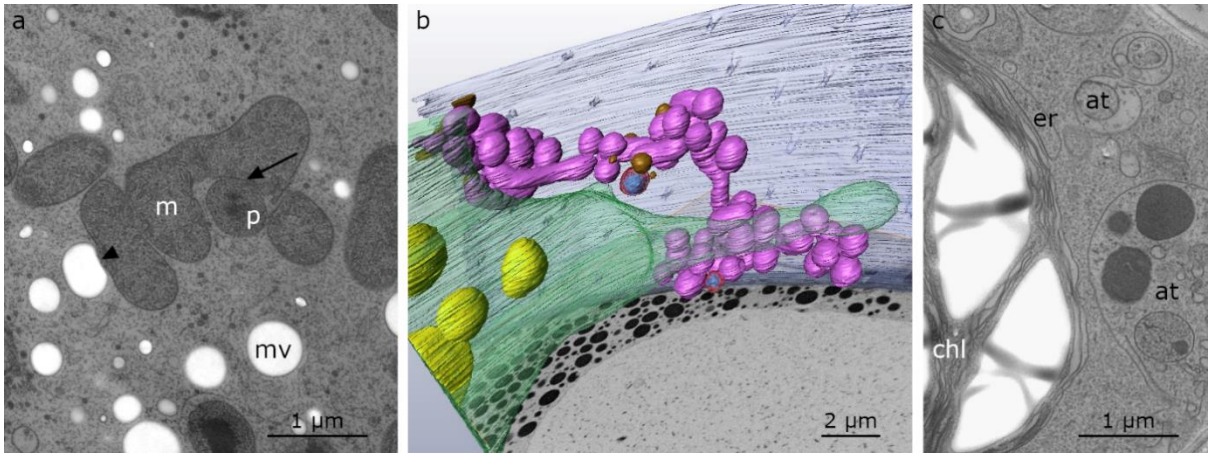

Figure 1. a) TEM micrograph of chilled *Micrasterias denticulata* cell (+4 °C, 3 weeks), depicting elongation, aggregation and fusion of mitochondria (m) and contact to a mucilage vesicle (mv, arrowhead) and a peroxisome (p, arrow). **b)** FIB-SEM reconstruction of extracellularly frozen (-2 °C) *M. denticulata* cell, visualizing extended mitochondrial network (purple) with contact to mucilage vesicles (brown) and peroxisomes (blue crystal in transparent red). The reconstruction also visualizes the chloroplast (transparent green) with starch grains (yellow) and the cell wall (transparent blue). **c)** TEM micrograph of extracellularly frozen (-2 °C) *Lemna* sp., depicting numerous autophagic structures (at) and bloated ER (er) and thylakoids of the chloroplast (chl).

References:
[1] M Stamenkovic *et al*, Protoplasma 251 (2014) p. 1491-1509
[2] JJ Sauter *et al*, J Plant Physiol 149 (1996) p. 451-461
[3] LV Gusta *et al*, Physiol Plant 147 (2013) p. 4-14
[4] M Wisniewski *et al*, Crit Rev Plant Sci 33 (2014) p. 92-124

This research was funded by the Austrian Science Fund, grant number P30139-B32 to Gilbert Neuner. The authors dedicate this work to the life of Ursula Lütz-Meindl (1956*-2020†).

POSTER

Interferometric cathodoluminescence in (S)TEM

Michael Stöger-Pollach[1], Stefan Löffler[1], Cornelia F. Pichler[2], Leo Stöger[2] and Niklas Maurer[2]

1 USTEM, TU Wien, Vienna, Austria
2 Institute for Solid State Physics, TU Wien, Vienna, Austria

Cathodoluminescence – CL – in a (scanning) transmission electron microscope – (S)TEM – is attracting more and more interest since the advent of effective CL detectors. Nevertheless, the sample geometry is such, that the specimen may act as a light guide, because of its limited thickness required for being electron transparent. Hence, interference effects of partial inner reflection at the top and bottom sample/vacuum interfaces or interfaces being parallel to the electron beam axis influence the detected CL signal.

In the present study we show investigate Silicon, GaAs, GaN and MgO for demonstrating the alteration of the spectra caused by interferometry of Cerenkov light being emitted, as soon as the velocity of the probe electron exceeds the phase velocity of light inside the specimen.

For Silicon [1] we demonstrate, how strong interference influences the measured signal. In the case of GaAs we demonstrate that the interference effects are able to suppress the CL signal in the IR region stemming from the de-excitation at the band edge. In the case of GaN the same is proven, but for the UV region.

In the case of MgO we make use of it and determine the refractive index with respect to the wave length for visible light, because its band gap is large enough for being transparent for light [2].

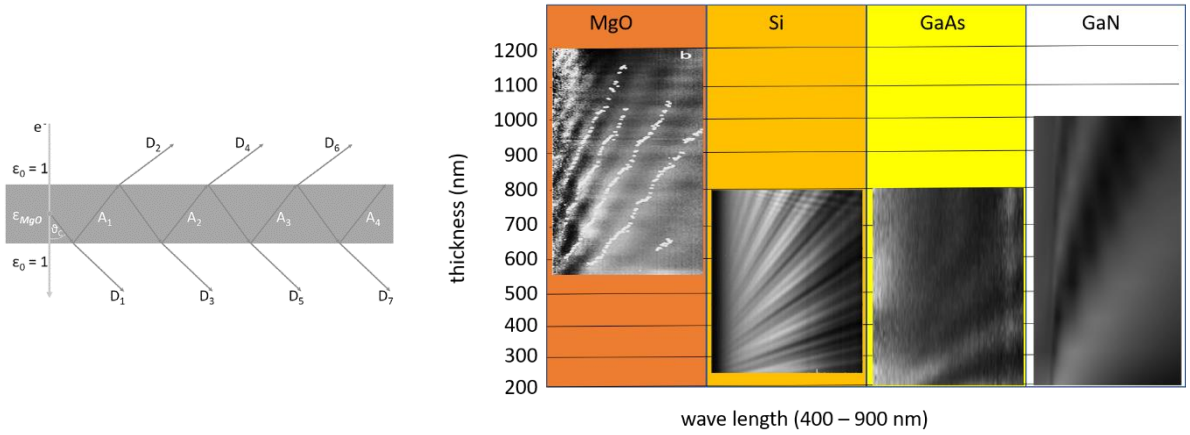

Figure 1. a) Schematic of interference of Cerenkov light inside a slab-like specimen. **b)** Interferometric CL spectra of MgO, Si, GaAs and GaN with respect to sample thickness in a range from 400 nm to 900 nm wavelength, each.

References:
[1] M Stöger-Pollach *et al*, Ultramicroscopy **200** (2019) p. 111-124
[2] M Stöger-Pollach *et al*, Ultramicroscopy **214** (2020) p. 113011 1-5

This research was in part supported by the SINNCE project of the European Union's Horizon 2020 programme under the grant agreement No. 810626.

Higher moments in DPC

Stefan Löffler[1], Dominik Boya[2] and Michael Stöger-Pollach[1]

1 University Service Centre for Transmission Electron Microscopy, TU Wien, Wien, Austria
2 Institute of Solid State Physics, TU Wien, Wien, Austria

Differential Phase Contrast (DPC) is a versatile method for measuring a sample's electromagnetic (EM) fields [1]. From this, charge densities can be derived, which in turn can improve light-element sensitivity and signal-to-noise ratio [2]. The underlying principle behind DPC is that an EM field changes the electron beam's momentum distribution, which is directly reflected in the diffraction plane. Conventionally, one quantifies the shift of $\langle p_i \rangle$, the center-of-mass (COM) of the diffraction pattern in a STEM geometry, to derive the EM fields by employing Ehrenfest's theorem [3].

However, the diffraction pattern is not fully described by a simple shift (fig. 1). For that reason, we investigate the significance of higher moments of the momentum distribution (such as its standard deviation). From a quantum-mechanical derivation, it can be shown that the second moment ($\langle p_i p_j \rangle$, which can be calculated directly from the diffraction pattern) is related to the outer product of the electric field with itself. This allows to infer the (average) gradient of the E-field and, consequently, construct a quadratic approximation of the potential. In a similar way, even higher moments can be determined as well, provided the signal-to-noise ratio is good enough.

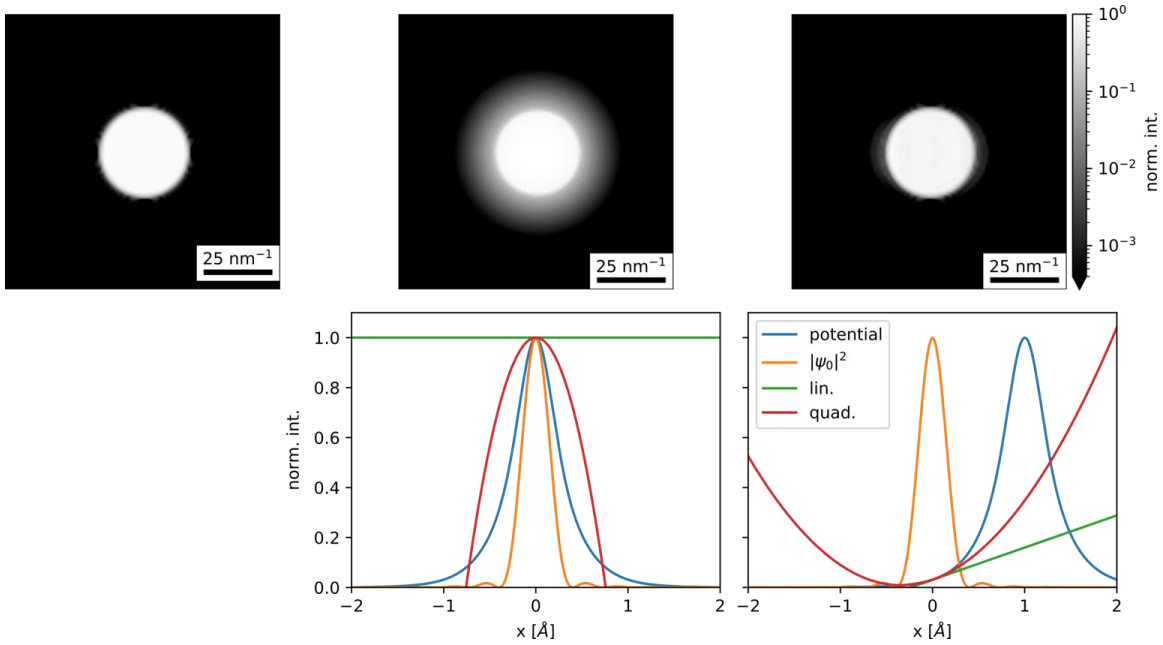

Figure 1. Simulations for an atomic column with 4 Si atoms using 300 keV and a convergence semi-angle of 30 mrad. Left: vacuum, middle: beam on the atomic column, right: beam close to the atomic column. Top: diffraction patterns, bottom: line profiles through the electrostatic potential, the beam intensity $|\psi_0|^2$, the linear approximation to the potential using $\langle p_i \rangle$, and the quadratic approximation using $\langle p_i p_j \rangle$.

Calculating the E-field's gradient can be done automatically from the same datasets used for DPC when using pixelated detectors. As such, it allows to obtain additional information from already existing data to reduce the required number of scan points, improve the precision of the E-field measurement, and to better characterize the sample.

References:
[1] K Müller *et al*, Nature Communications **5** (2014) p. 5653.
[2] I Lazić, E G T Bosch and S Lazar, Ultramicroscopy **160** (2016), p. 265.
[3] P Ehrenfest, Zeitschrift für Physik **45** (1927), p. 455.

SL acknowledges financial support by the Austrian Science Fund (FWF) under grant nr. I4309-N36.

Transmission Electron Microscopy Lab for Nano-Imagining and –Analytics of Functional Solid State and Biological Materials (BioMat-TEM).

Gregor A. Zickler[1], Astrid Obermayer[2], Nicole Meisner-Kober[2], Gilles R. Bourret[1] and Simone Pokrant[1].

1 Department of Chemistry and Physics of Materials, Paris-Lodron University Salzburg, Salzburg, Austria
2 Department of Biosciences, Paris-Lodron University Salzburg, Salzburg, Austria

The core facility electron microscopy (EM) of the Paris Lodron University Salzburg hosts a scanning electron microscope (SEM) and a 200 kV cold field emission gun transmission electron microscope (TEM) both equipped with EDX detectors. It supports around 90 researchers and 70 PhD students in the field of material science, solid-state chemistry, solid-state physics, mineralogy, biology and medicine by providing compositional and structural analytics down to sub-nanometer scale.

In the last years, the focus on biomedical research became stronger in Salzburg fuelled by excellence clusters in e.g. cancer or extracellular vesicle research with additional funding by the Land Salzburg. Imaging biological structures beyond the limit of light microscopy in their native environment in close-to-live conditions at the nanoscale is essential for the investigation of structure-function relationships relevant for biomedical research.

The material science community in Salzburg is internationally recognized for research and development of functional materials and devices, where a detailed understanding of the electronic structure is crucial, in addition to morphological and compositional information, in order to determine structure-property relations on the nanoscale.

To further leverage these successful research areas, there is an urgent need for high contrast imaging and electronic structure assessment on the nanoscale under low dose/cryo conditions for biological and material science samples in Salzburg, especially since these possibilities are missing in the west of Austria. Equipping the existing TEM with a cryo sample preparation and transfer unit, a cryo holder, an improved camera system and an electron energy filter, financed by an FFG infrastructure call project, will enable cryo imaging and electronic structure characterisation of beam sensitive samples.

In the start-up phase, standard operation procedures for cryo sample preparation and (high contrast) imaging of biological samples and for the assessment of electronic structures of functional materials and devices will be developed. These processes are linked not only by using the same infrastructure, but also by the common goal to inflict as little sample damage as possible. Beyond enabling state of the art applications in both material science and biological research, we expect additional breakthrough in 1) the morphological analysis of very beam sensitive solid-state samples like aerogels and 2) the combination of structural with compositional analysis of biological materials such as extracellular vesicles at the nanoscale. Upon project implementation, this investment will result in opportunities for follow-up projects and high impact publications in material science and biomedical research in Salzburg.

Acknowledgement:

The authors acknowledge funding for the project BioMat-TEM from the F&E-Infrastrukturförderung, FFG.

3D - HREM examination of dermal vessels in in a healthy donor

Plamena Mincheva, Paata Pruidze, Atieh Seyedian Moghaddam, Stefan H. Geyer, Wolfgang J. Weninger

Medical University of Vienna, Centre of Anatomy and Cell Biology, Division of Anatomy, Vienna, Austria

High Resolution Episcopic Microscopy (HREM) has been successfully utilised to study the dermal arteries of thick skin in the human finger pad [1]. The aim of this project was to explore if HREM derived data is also suitable to analyse the topology of the dermal blood vessels in thin skin of the human lower limb.

Tissue samples were taken from the skin region parallel to the collum fibulae of a human body donor and were harvested using 4 mm biopsy punches. Samples were fixed in 4% PFA/PBS and embedded for HREM data generation following existing protocols [2]. HREM-volume data sets with voxel sizes of 1.48 x 1.48 x 1.5 μm^3 were generated. Data sets consisted of image stacks comprising about 3000 single images. The dermal arteries were manually segmented using the software Amira (Version 2020, Thermo Scientific). Three-dimensional surface rendered models, volume rendering and virtual re-section tools of Amira were used for analysing the data.

HREM data provided enough quality to identify larger arteries and veins of the profound plexus at the border of dermis and subcutis. Ascending dermal arteries could be manually traced through the volume data set and exhibited tree-like ramifications. HREM data provided also sufficient detail to detect small arteries, capillaries and arterio-arterial anastomoses.

Our results demonstrate that HREM is capable to visualize the vessels in thin skin. Though the generation of surface rendered models necessitates manual segmentation and is therefore time-consuming, our study shows that HREM-data contribute to a better understanding of the architecture of the dermal blood vessels.

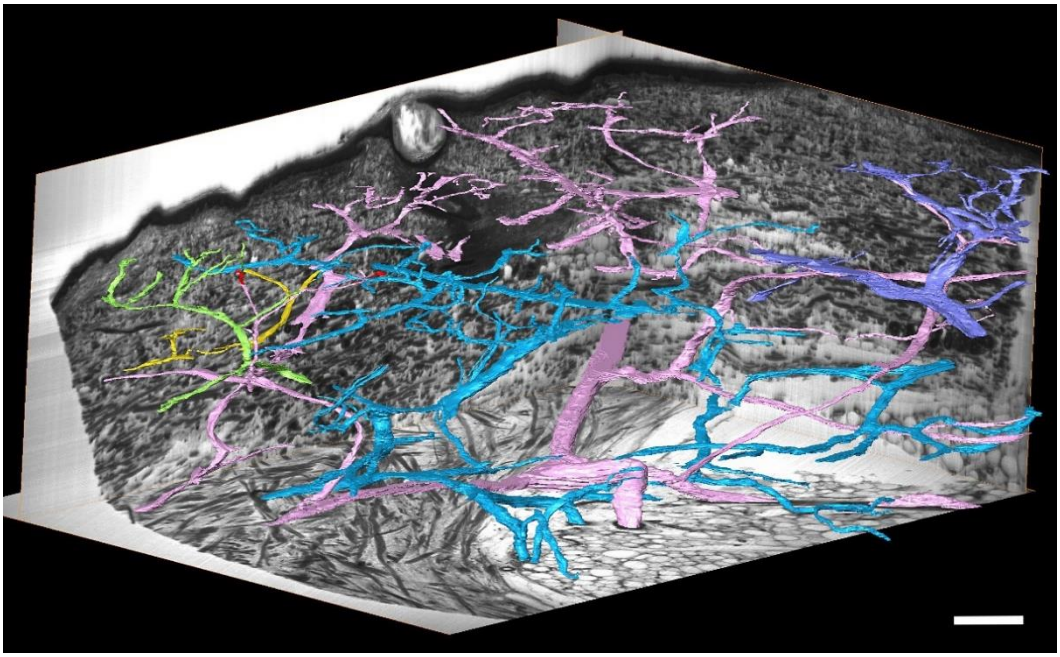

Figure 1. Surface rendered 3D model of the dermal vessels of a thin skin biopsy. Scalebar 250 µm.

References:

[1] SH Geyer, MM Nohammer, IE Tinhofer, WJ Weninger, J Anat, **223** (2013)
[2] WJ Weninger, SH Geyer, TJ Mohun, et al., Anat Embryol (Berl) **211** (2006)

IR vs. Raman microscopy – Comparison, Synergies and Practical Guidelines

Herbert Kobald[1], Alexander Kobald[1], Claudia Mayrhofer[2] and Harald Fitzek[1,2]

[1]Institute of Electron Microscopy and Nanoanalysis, NAWI Graz, Graz University of Technology, Steyrergasse
[2]Graz Centre for Electron Microscopy, Steyrergasse 17, Graz, Austria

We have compared Raman microscopy with the two main types of IR microscopy (Transmission, Attenuated Total Reflection) on five samples representing the typical areas of application, namely a packaging foil (polymers), a cigarette filter (particles), a paracetamol tablet (pharmaceuticals), a coated wood (biological materials) and a high-quality paper (organic-inorganic composite). Our goal is to give practical guidelines for the best choice of technique for any given application as well as highlight possible synergies from using more than one technique on the same sample.

IR and Raman microscopy are widely used techniques that are both based on vibrational spectroscopy. From a vibrational spectroscopic point of view, they yield complementary information due to their different selection rules, sensitivity to various compounds and limitations with regard to spectra range and background [1]. From a microscopic point of view (especially a practical one) the techniques have quite distinct advantages as well. The standard confocal Raman microscopy has a higher resolution, simpler sample preparation/handling and more versatility, whereas the usual IR microscopy methods (ATR, Transmission) have higher measurement speeds and fewer background problems. We are discussing 3 questions in this work (for a given sample/ experimental situation): *Which of the three microscopy techniques (confocal Raman, ATR-IR or Transmission-IR) is most practical? Which yields the most information? Is there an advantage of using more than one technique?*

Figure 1 shows as an example the Raman measurement from the coated wood. We see very good image quality but three particles are marked that could not be identified by Raman due to high fluorescence. These particles were later identified as grease and human hair contaminations by the complementary IR-ATR microscopy (results not shown). As is evident from this example, the choice between Raman, IR-ATR and IR-transmission depends on many factors and we aim to provide some intuition about which method is best suited for your sample and when a combination of several techniques is beneficial.

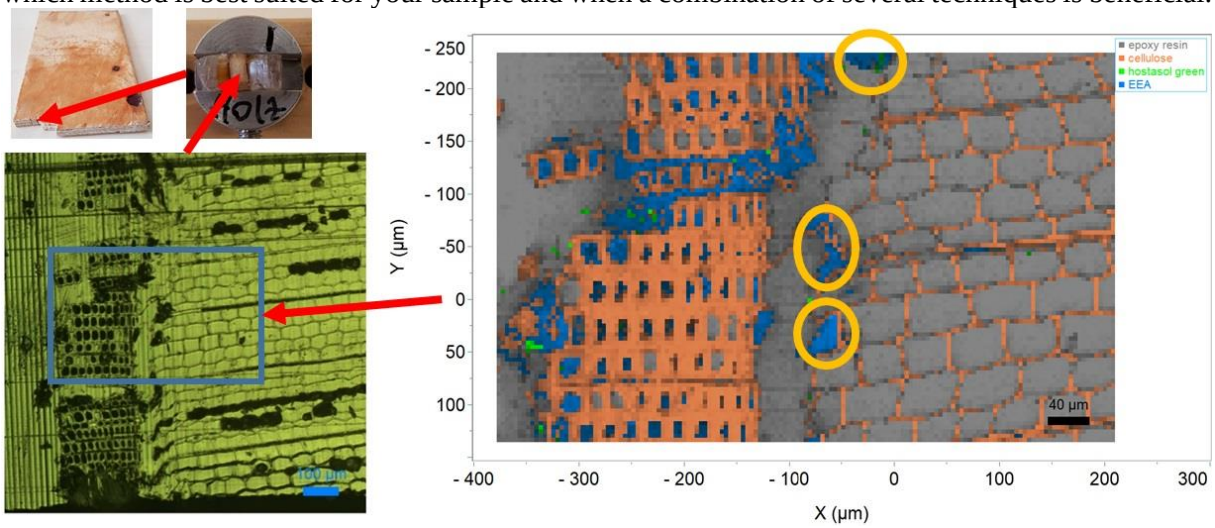

Figure 1: Results of the Raman mapping on the coated wood sample (right) and macroscopic/microscopic image of the sample (left top/bottom). Note that the regions marked with yellow circles show low signal to noise ratios and high fluorescence in the Raman measurement**.**

[1] Larkin, P. (2017). *Infrared and Raman spectroscopy: principles and spectral interpretation.* Elsevier.
[2] Long, D. A. (2002). *The Raman effect: a unified treatment of the theory of Raman scattering by molecules.* John Wiley & Sons

Quantifying Cellular Responses to Stress in *Saccharomyces cerevisiae*

Katharina Keuenhof[1], Lisa Larsson Berglund[1,2], Kara L Schneider[2], Sandra Malmgren Hill[3,4], Per O Widlund[2], Thomas Nyström[2], Johanna L Höög[1]

1 Department of Chemistry and Molecular Biology, University of Gothenburg, Sweden
2 Department of Microbiology and Immunology, Institute of Biomedicine, The Sahlgrenska Academy at the University of Gothenburg, Sweden
3 Department of Psychiatry and Neurochemistry, Institute of Neuroscience and Physiology, The Sahlgrenska Academy at the University of Gothenburg, Sweden
4 Department of Medical Genetics, Cambridge Institute for Medical Research, United Kingdom

The presence of established mechanisms to cope with stressors is essential for survival in all species on earth. One of the ways stress-induced changes in and of cellular components can manifest is through disease, for example proteinopathies such as Parkinson's, Alzheimer's and Huntington's. Those ageing-related diseases can be studied using the budding yeast *Saccharomyces cerevisiae* as model organism [1]. Using heat-shock, a significant challenge for all living organisms, and replicative ageing, it is possible to gain insight into the cellular architectural changes involved. Although the stress response, especially to temperature shifts, is well characterized at the molecular level, there is no comprehensive and quantitative model for structural changes within the cell.

Using transmission electron microscopy of thin (70 nm) sections of high-pressure frozen yeast cells (Figure 1), we have imaged thousands of cells in different stages of heat-shock and thoroughly examined structural changes over time. We have quantified the size, number and location of most organelles and some of their contact sites. We measured an increase in the volume of cells, mitochondria, vacuoles, lipid droplets, and an enlargement of organelle contact sites in heat-shocked cells. Additionally, we have detected and quantified the appearance of electron-translucent structures that increasingly spread in the cytoplasm as heat-shock progresses [2].

Similarly, by performing electron tomography on thick (350 nm) serial sections of young and old high-pressure frozen yeast cells, we are reconstructing entire yeast cells at nanometre-resolution. This allows us the model organelles and their contact sites within the entire cell and observe potential changes in cellular ultrastructure.

An unbiased classification and quantification of structural cellular changes creates new maps of the internal organization of the cell during cellular stress and unexpected changes can now be further investigated using molecular cell biology and genetics. This can unravel potentially uncharacterized cellular stress response mechanisms or bring new light to already described pathways.

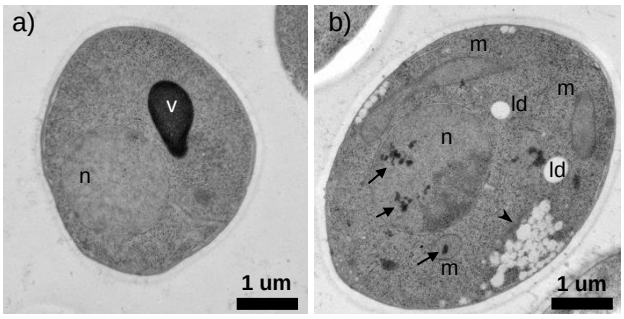

Figure 1. a) Budding yeast cell at 30°C. **b)** Budding yeast cell after 90 min at 38°C heat-shock. n: nucleus, v: vacuole, m: mitochondria, ld: lipid droplet, arrows: electron-dense content, arrowhead: electron-translucent clusters.

References:
[1] S Tenreiro *et al*, Journal of Neurochemistry 127 (2013), p. 438-452.
[2] K Keuenhof *et* al, biorxiv (2021).

We would like to thank Claes Andreasson, Sabrina Büttner. Martin Ott, Mattia Donà, Eileen O'Toole, and Gary Morgan for valuable and input and support during the realisation of this project.

Staying "Cool" under Agitation: An Improved Freeze Substitution Protocol for Preservation of Cryofixed Carnivorous Plant's Glands

Sabine Dürr[1], Irene K. Lichtscheidl[1] and Siegfried Reipert[1]

1 Core Facility Cell Imaging and Ultrastructural Research, University of Vienna, A-1090 Vienna, Austria

Depicting the rapidly cryoimmobilized ultrastructure of resin-embedded tissues via Transmission Electron Microscopy (TEM), potentially, enables studying of cellular processes on basis of snapshots at nanometre scale. To succeed with such an approach, freezing, low-temperature dehydration and fixation of the frozen tissues have to be adapted to the requirements of the tissue in question.

We established a cryopreparation protocol that suits comprehensive ultrastructural studies of various glands associated with leaves of the carnivorous plant *Pinguicula vulgaris*. Also known as "common butterwort", this plant attracts, catches, absorbs and digests nutrients from small insects [1]. Surprisingly little is known about the ultrastructural adaptations of their glands to carnivorous function in this genus. Therefore, we tested the feasibility of cryopreservation for structures related to secretion and digestion by freezing with a high-pressure freezer HPM100 (LEICA Microsystems) followed by freeze substitution accelerated by sample agitation in an automated freeze substitution unit, AFS2 (LEICA Microsystems).

On one hand it turned out that agitation overnight completed the substitution process in OsO_4/ acetone timely, as it did for other applications of the agitation module, Fig. 1A, in the past [2]; on the other hand, it resulted in poorly contrasted, washed-out tissues unsuitable to address the questions outlined above. Therefore, we designed a substitution protocol combining low-temperature substitution with 0.1% tannic acid, with low-temperature osmification and stabilization of the ultrastructure with glutaraldehyde. Such a protocol required prolonged processing under agitation and repeated washing steps with precooled acetone in between media changes. At the end, this addition effort payed off, since the embedded *P. vulgaris* showed much improved preservation of cellular aspects of gland tissues, as demonstrated in Fig. 1C.

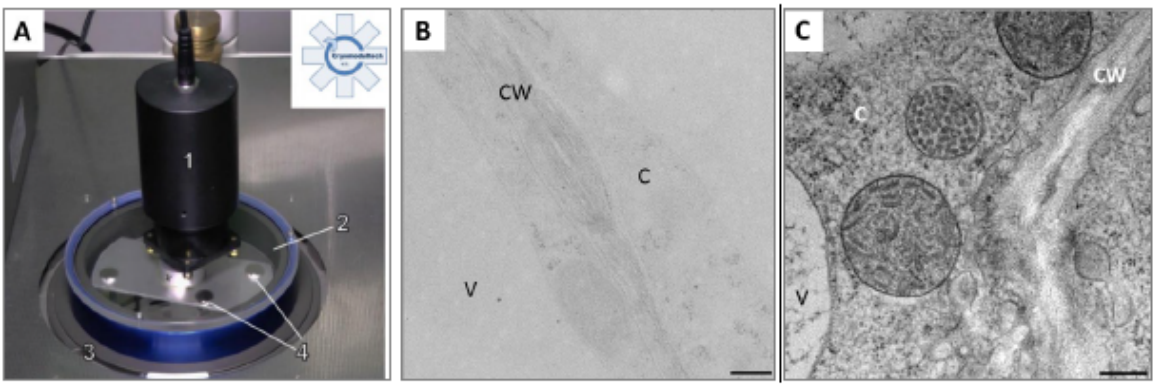

Figure 1. A) Agitation module. **B)** Standard freeze-substitution protocol **C)** Prolongated and refined freeze-substitution protocol. Membranes and cell wall of a digestive gland are depicted in high contrast. Vacuole (V), cell wall (CW), cytoplasm (C). Scale bar indicates 250 nm.

References:
[1] Legendre L. Acta Bot. Gallica **147** (2000), p. 77-95.
[2] Goldammer H. *et al*, Protist **167/4** (2016), p. 369- 376.
[3] Reipert S. *et al.* J Histochem Cytochem **66/12** (2018), p. 903-921

We gratefully acknowledge financial support by the "Hochschuljubiläumsstiftung Stadt Wien" (code H-281616/2020).

3D TEM analysis reveals interaction surface of ER and Endo-Lysosomes in RBL-1 immune cells

Philip Steiner[1], Ancuela Andosch[2], Karin Oberascher[2], Hubert Kerschbaum[2] and Susanna Zierler[1]

1 Institute of Pharmacology, Medical Faculty, Johannes Kepler University, Linz, Austria
2 Department of Biosciences, Paris Lodron University, Salzburg, Austria

Rat basophilic leukemia cells (RBL) are often used as a model for primary mast cells. Basophils and mast cells are innate effector cells of allergic reactions [1, 2]. Previously, we reported that the two-pore channel, TPC1, plays an important role in the Ca^{2+} homeostasis of intracellular organelles, such as the endo-lysosomal compartment and the endoplasmic reticulum (ER) of RBL-1 cells and primary murine mast cells. Pharmacologic inhibition or genetic ablation of TPC1 results in enhanced anaphylactic responses [2]. However, there is a lack of ultrastructural knowledge that underlies these processes. We have therefore implemented 2D and 3D transmission electron microscopic (TEM) methods after high pressure freeze fixation to investigate the ultrastructure of RBL-1 cells (Fig. 1a). Our 2D and 3D TEM investigations depict that ER and endo-lysosomes are in close spatial proximity (Fig. 1b-c). It appears that this proximity increases with later stages of endo-lysosomes and lysosomes that are closer to the nucleus and is not observable in early endosomes near the plasma membrane. Endosome-ER contact sites have been examined for their 2D ultrastructure with regard to their Ca^{2+} signalling before [4]. However, only 3D TEM tomography reveals the extent of contact surface between the two organelles (Fig. 1c). Our results will be compared with RBL-1 cells, treated with the plant alkaloid tetrandrine. It was reported before that tetrandrine acts as an inhibitor of TPCs [2, 3]. We therefore assume a significant ultrastructural distinction of ER and endolysosomal interaction in comparison to untreated RBL-1 cells. Moreover, electron energy loss spectroscopic- (EELS) or energy dispersive X-ray (EDX) analysis could provide more information on the intracellular and interorganellar Ca^{2+} composition. In summary, we aim at a better understanding of the role of TPC channels in the regulation of the crosstalk between ER and endo-lysosomes at an ultrastructural level. Correlating our findings with molecular biological and immunological experiments could help clarify whether TPC channels indeed are promising pharmacological targets for the treatment of allergic hypersensitivity.

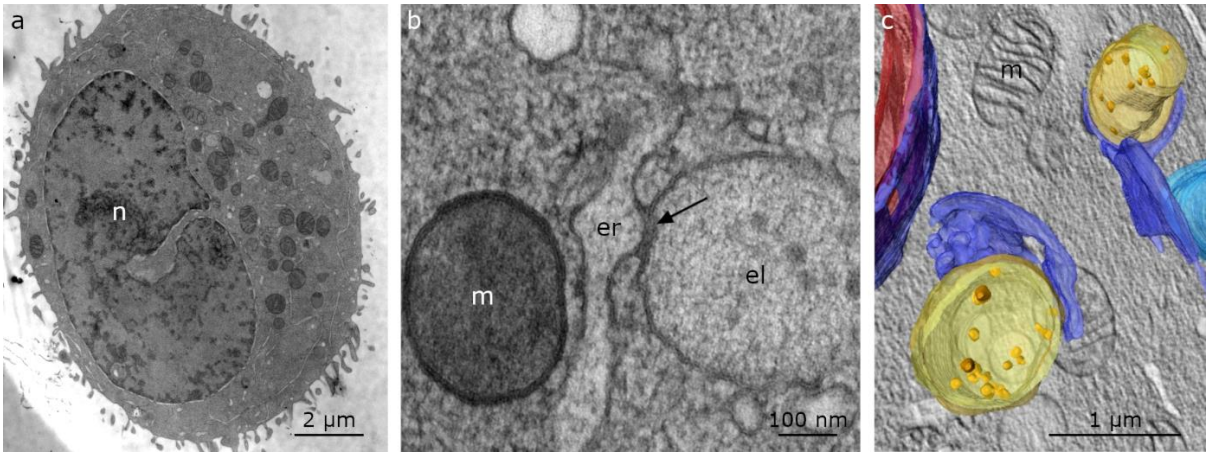

Figure 1. a) 2-D TEM overview of RBL-1 cell, depicting the pleomorphic nucleus (n). **b)** 2-D TEM micrograph of RBL-1 cell, indicating the proximity of a mitochondrion (m) to the endoplasmic reticulum (er) and the contact site (arrow) of the ER (er) and an endolysosome (el). **c)** 3-D TEM tomogram of RBL-1 cell visualizing the ER envelope (blue) around endolysosomes (yellow) in the vicinity of the nucleus (red).

References:
[1] J-M Yoo *et al*, J Med Food 17(1) (2014) p. 92-102
[2] E Arlt *et al*, PNAS 117(30) (2020) p. 18068-18078
[3] Y Sakurai *et al*, Science 347 (2015) p. 995-998
[4] BS Kilpatrick *et al*, Cell Rep 18 (2017) p. 1636-1645


JKU
Zentrum für
Oberflächen-
und Nanoanalytik


Austrian Society for
ASEM
Electron Microscopy